

**FINAL REPORT
(DE-FG-22-94PC94120)**

**Investigation of The Effect of Coal Particle Sizes on the Interfacial and
Rheological Properties of Coal-Water Slurry Fuels**

Research Period: July 1, 1994 - June 30, 1996

submitted to:

**U. S. Department of Energy
Pittsburgh Energy Technology Center
P. O. Box 10940
Pittsburgh, Pennsylvania 15236-0940**

**RECEIVED
USDOE/PEETC
26 OCT 17 AM 8:41
ACQUISITION & ASSISTANCE DIV.**

by

**PI: Ken D. Kihm, Ph.D., P.E.
Associate Professor in Mechanical Engineering
Texas A&M University
College Station, Texas 77843-3123**

MASTER

October 1996 DISTRIBUTION OF THIS DOCUMENT IS UNLIMITED
ln

**CLEARED BY
PATENT COUNSEL**

ACKNOWLEDGMENT

This report was prepared with the support of the U.S. Department of Energy-Pittsburgh Energy Technology Center, Grant No. DE-FG-22-94PC94120 under technical monitoring from Dr. Soung S. Kim at the Coal Utilization Division. However, any opinions, findings, conclusions, or recommendations expressed herein are those of the author and do not necessarily reflect the view of DOE.

DISCLAIMER

Portions of this document may be illegible in electronic image products. Images are produced from the best available original document.

DISCLAIMER

This report was prepared as an account of work sponsored by an agency of the United States Government. Neither the United States Government nor any agency thereof, nor any of their employees, make any warranty, express or implied, or assumes any legal liability or responsibility for the accuracy, completeness, or usefulness of any information, apparatus, product, or process disclosed, or represents that its use would not infringe privately owned rights. Reference herein to any specific commercial product, process, or service by trade name, trademark, manufacturer, or otherwise does not necessarily constitute or imply its endorsement, recommendation, or favoring by the United States Government or any agency thereof. The views and opinions of authors expressed herein do not necessarily state or reflect those of the United States Government or any agency thereof.

DOE/PC/94120--T8
FINAL REPORT
(DE-FG-22-94PC94120)

Investigation of The Effect of Coal Particle Sizes on the Interfacial and
Rheological Properties of Coal-Water Slurry Fuels

Research Period: July 1, 1994 - June 30, 1996

submitted to:

U. S. Department of Energy
Pittsburgh Energy Technology Center
P. O. Box 10940
Pittsburgh, Pennsylvania 15236-0940

by

PI: Ken D. Kihm, Ph.D., P.E.
Associate Professor in Mechanical Engineering
Texas A&M University
College Station, Texas 77843-3123

October 1996

MASTER

ABSTRACT

The scope of the project is two fold: (1) examining particle size effect on interfacial properties of CWS fuels by measuring static and dynamic surface tension properties of specially prepared CWS samples containing different ranges of coal particle sizes, and (2) studying the effect of particle size on CWS atomization characteristics by measuring mean diameters of several different CWS sprays generated by sonic air blasting.

The results show that both static and dynamic surface tensions decrease with increasing coal particle size and mean droplet diameter of CWS sprays also decreases with increasing coal particle size. Based on the experimental evidence we conjecture that three different energies are competing in slurry atomization: (1) the internal capillary holding between particles and water, (2) the interfacial surface tensile energy at the slurry surface contacting air, and (3) the external air blast shear energy acting against the former two energies. The internal capillary holding force decreases with increasing particle size. This force is believed to play a major role in determining the effect of particle size on CWS atomization.

TABLE OF CONTENTS

<u>Contents</u>	<u>Page</u>
Abstract	1
Table of Contents	2
Chapter 1 Introduction	3
Chapter 2 Objectives	5
Chapter 3 Effect of Coal Particle Size on CWS Surface Tension Properties	6
3.1 CWS Sample Preparation	6
3.2 Static CWS Surface Tension	8
3.3 Dynamic CWS Surface Tension	12
3.3.1 Maximum bubble pressure technique	12
3.3.2 Modification of the Kruss tensiometer	14
3.3.3 Detailed digitized output reading data	16
3.4 Effect of Coal Particle size on CWS dynamic surface tension	22
3.5 Concluding Remarks	22
Chapter 4 Effect of Coal Particle Size on CWS Atomization	26
4.1 CWS Sample Preparation	26
4.2 Experimental Setup for Sonic Airblast Atomization	29
4.3 Preliminary Measurements Using Aqueous Solutions	31
4.4 Effect of Coal Particle Size on CWS Atomization	31
4.5 Concluding Remarks	42
Chapter 5 Summary and Conclusion	47
Chapter 6 Suggestion for Future Research	48
References	49
List of Publications under the US-DOE Support	50

Chapter 1 Introduction

Coal-water slurry atomization involves interactions between three different phases: solid (coal particles), liquid (water and additives), and gas (air or steam). Surface or interfacial tension is one significant property in determining atomization characteristics of liquid or slurry fuels. Under the quasi-equilibrium conditions of low shear-rates of excessively slow atomization, the static surface tension of the fluid is an appropriate measure of the fluid's ability to form small radius droplets. However, the surfactants, additives, or wetting agents presented in the CWS formulation do not reach an equilibrium concentration throughout the solid-liquid or liquid-vapor interfaces at higher shear rates. Therefore, dynamic surface tension should be a more appropriate measure in assessing the atomization that usually occurs at high shear rates.

The dynamic surface tension of a fluid is simply a measurement of the surface tension at a particular rate of surface formation or shear rate. The static and dynamic surface tension values are the same for pure fluids, such as water. The values of dynamic surface tension for slurry mixtures containing solid particles and various additives may be higher than the corresponding static surface tension because insufficient time exists for the migration of surfactant additives to the atomized interface from the bulk mixture. The difference increases between the two surface tension values at higher shear rates since less time is allowed for the surfactant migration.

It is the intention of the present work to examine the effect of coal particle sizes on CWS static and dynamic surface tension properties, and its atomization characteristics. Rheology shows that the slurry viscosity generally increases with decreasing mean particle size (Botsaris and Glazman, 1989). When particles suspended in the solution are dispersed with additives and/or solvents, they form adsorption or solvation layers on the particle surface that increase the effective volume (f) of the particle. This effective volume increase is particularly significant for

small particles and can explain the increase of the slurry viscosity with decreasing mean particle size.

Our literature survey shows that no particle size correlations for surface tension, whether static or dynamic, and slurry atomization have been published. Examining particle size effect on interfacial properties of CWS fuels is attempted using specially prepared coal particle samples in different size ranges. We, then, studied the effect of particle size on CWS atomization characteristics to find the answers to two important questions that conform to the objective of the present project.

Chapter 2 Objectives

Objectives of the present study are to investigate the effects of coal particle size on CWS surface properties and its atomization characteristics. This report attempts to explore answers to two fundamental and important questions that have not been answered:

- (1) Do the static and dynamic surface tension properties of a CWS mixture increase or decrease with the suspended coal particle size?
- (2) What is the correlation between the coal particle size and the atomized CWS droplet size?
Will the average droplet size of CWS sprays increase or decrease with increasing coal particle size?

Chapters 3 and 4 will present our investigations and answer the above questions, respectively.

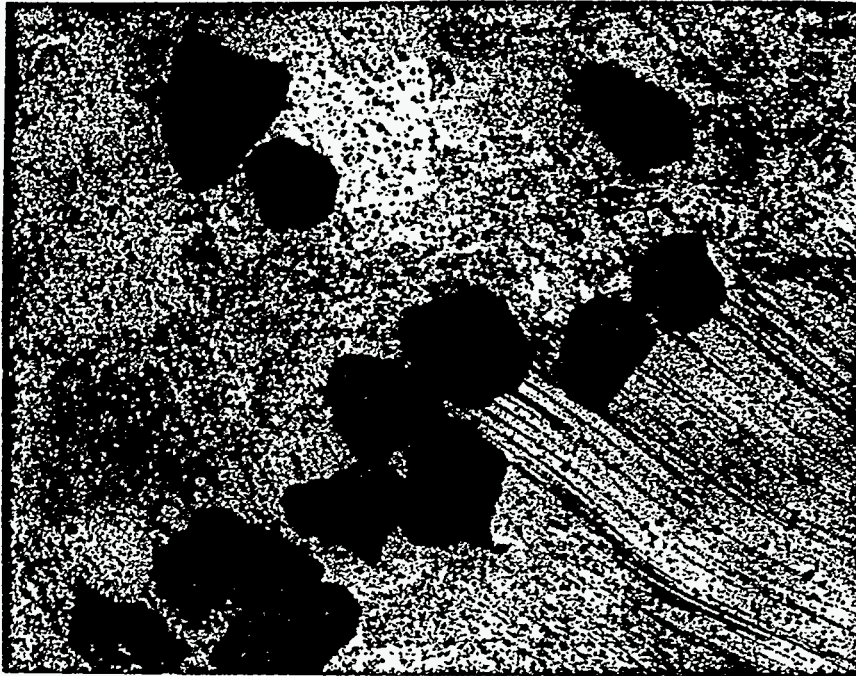
Chapter 3 Effect of Coal Particle Size on CWS Surface Tension Properties

We conducted experiments to investigate the effect of particle size on CWS surface tension properties. We obtained two different coal powder samples of different sizes through sieving of coal from the Upper Elkhorn Seam. The concentration of selected surfactants (anionic DDBS-soft, dodecylbenzene sulfonic acid) varied from 0-1.0% in weight while the coal loading remained at 40% in weight for all cases. A du Nouy ring tensiometer and a modified maximum bubble pressure tensiometer measured the static and dynamic surface tensions, respectively. The results show that both static and dynamic surface tensions increase with decreasing coal particle sizes suspended in CWS fuels.

3.1 CWS Sample Preparation

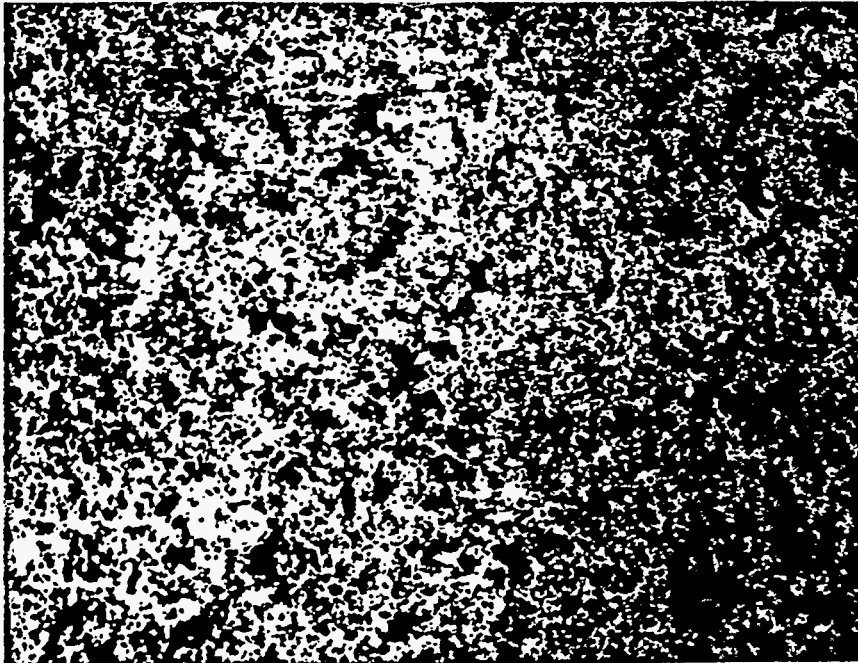
DOE-PETC provided the coarsely ground Upper Elkhorn Seam coal that was classified into several different size ranges using a sieve shaker at Texas A&M University. To reduce coal oxidation during sieving, the sieve array was sealed with tape and the duration of sieve shaking was kept at a minimum. In most cases, the sieving was completed within thirty minutes. Two samples were selected for testing so the effect of particle size on surface tension values could be distinctively observed. The medium sample contained coal particles between 180 and 250 μm (Fig. 3.1-a), and the fine sample contained coal particles less than 63 μm (Fig. 3.1-b).

A rotating mixer, running for twelve to twenty-four hours, completely mixed the coal and water with the basic additive of 0.5% Flocon. The specified amount of surfactant was then added and mixed by a magnetic stirrer for five minutes. The present experiments used 40% weight CWS fuels. The slurry viscosity increases with an increasing ratio of the packing density, defined as the ratio of the solid volume fraction to the maximum attainable solid volume fraction, i.e., f/f_m (Botsaris and Glazman, 1989). The uniform size distribution of the sieved coal



$180 \mu\text{m} < d < 250 \mu\text{m}$

(a)



$d < 63 \mu\text{m}$

(b)

Fig. 3.1 Electron microscope photographs of coarse and fine coal particle samples.

particles reduces the maximum attainable solid volume fraction and increases the packing density compared with coal powder of a wide size distribution. The 50% or higher weight CWS fuel samples were too viscous and the tensiometers could not function with acceptable accuracy.

3.2 Static CWS Surface Tension

A du Nouy ring tensiometer measured static surface tension for the coarse and fine CWS samples. Results are shown for 1840-x in Fig. 3.2 and for DDBS-soft in Fig. 3.3. For both surfactants, the static surface tension decreases with an increasing surfactant concentration and approaches a saturated value beyond a certain surfactant concentration, which is called a critical micelle concentration (CMC). The fine CWS sample shows larger surface tension values than the coarse sample, and the CMC of the fine CWS is higher than the coarse CWS.

The dashed arrows show the CMC of the fine sample, the solid arrows represent the CMC of the coarse sample, and the empty arrows are for the CMC of an aqueous solution of the specified surfactant. The CMC values for CWS fuels are higher than their aqueous counterparts. We believe the primary reason for this is that the surfactant adsorption on the coal particle surfaces requires more surfactant than the aqueous solution (Fig. 3.4). The surface adsorption can also explain the higher CMC of the fine CWS compared with the coarse CWS. Smaller coal particles create more total surface area than larger particles for the same coal loading, which causes the overall surface adsorption of the surfactant to increase. This needs higher surfactant concentration for the saturated surface tension level and higher CMC. In addition, the higher number density of smaller particles can block the surfactant migration to the surface.

The CMC concentration values of the considered cases are higher than 0.1%. Therefore, the dynamic surface tension measurement is carried out for surfactant concentrations higher than

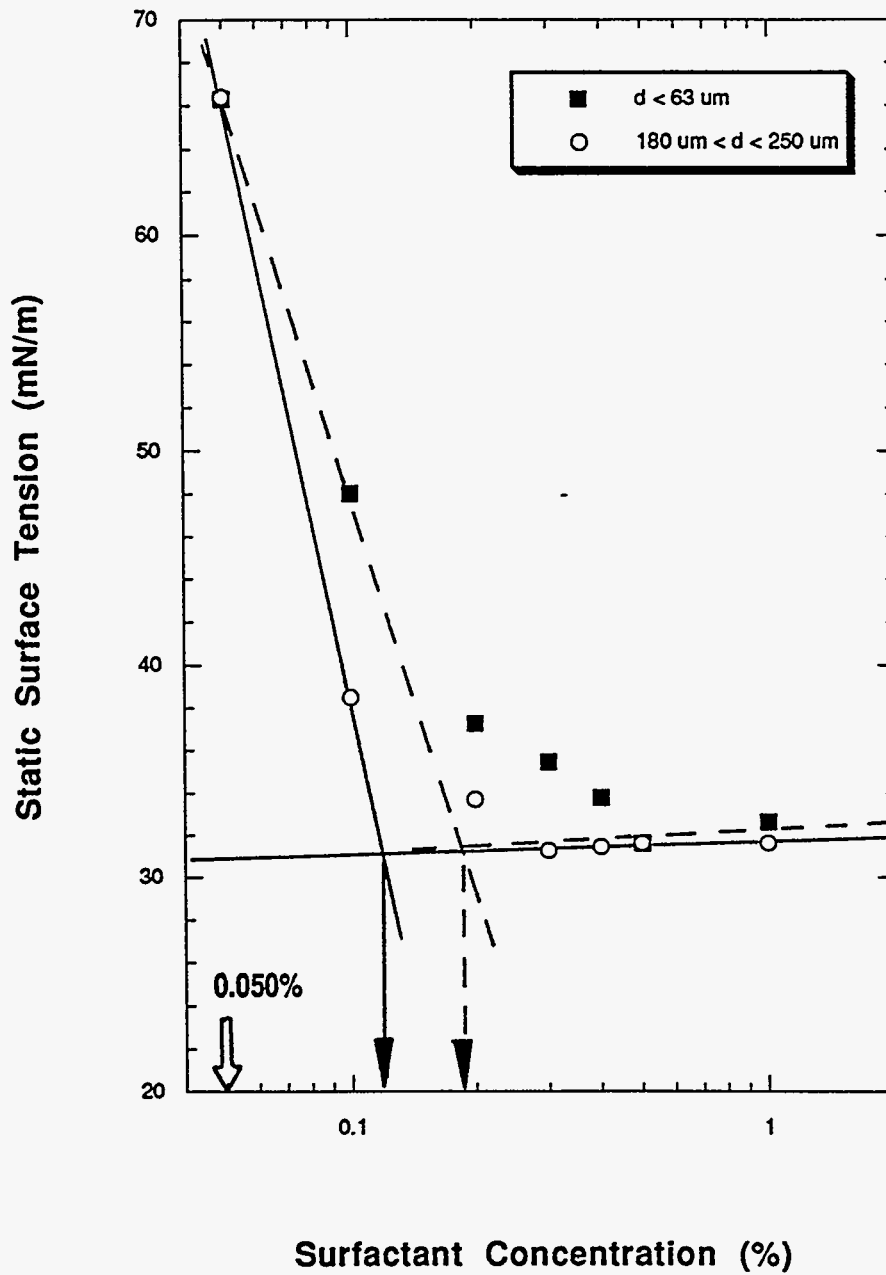


Fig. 3.2 Static surface tension versus concentration of 1840-x for 40% coal weight CWS fuels containing different particle sizes.

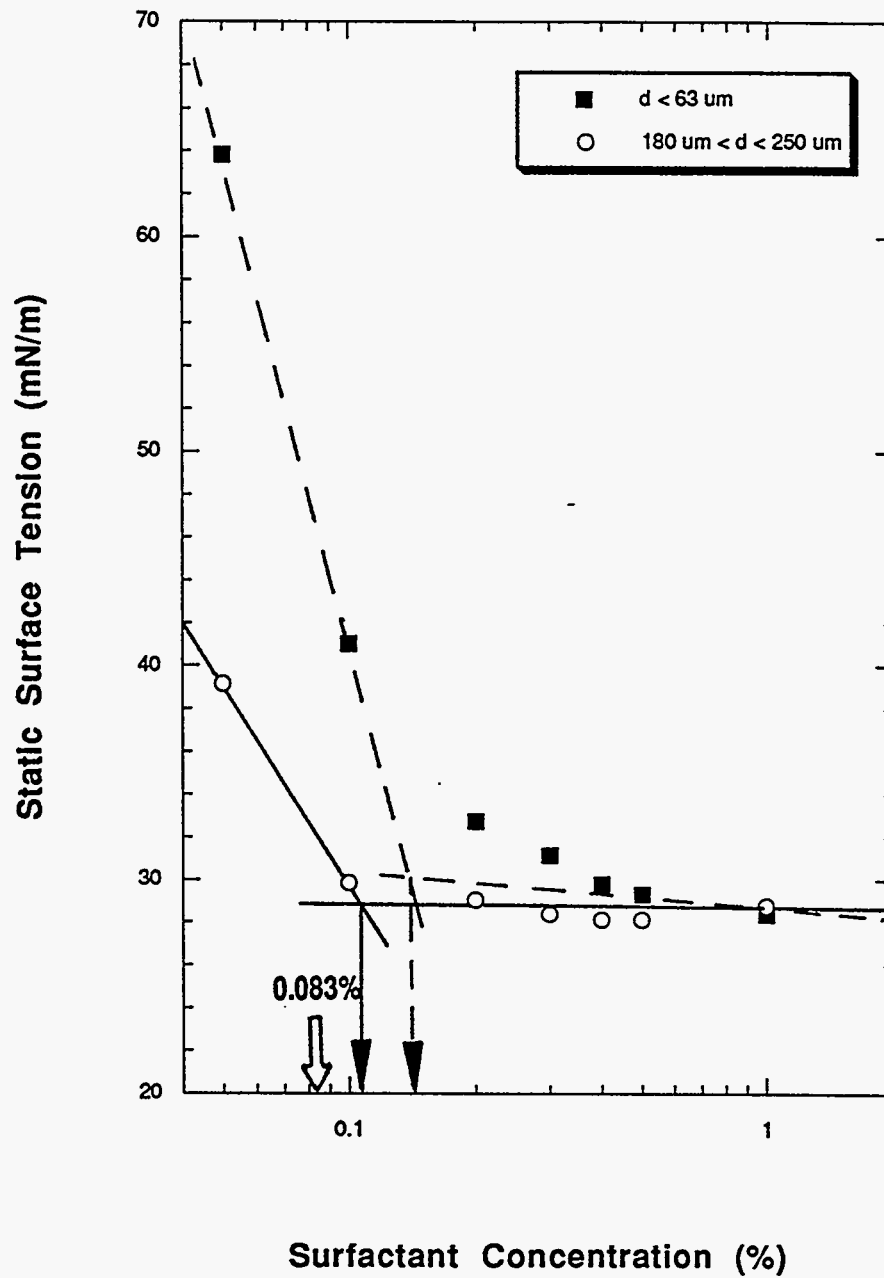


Fig. 3.3 Static surface tension versus concentration of DDBS-soft for 40% coal weight CWS fuels containing different particle sizes.

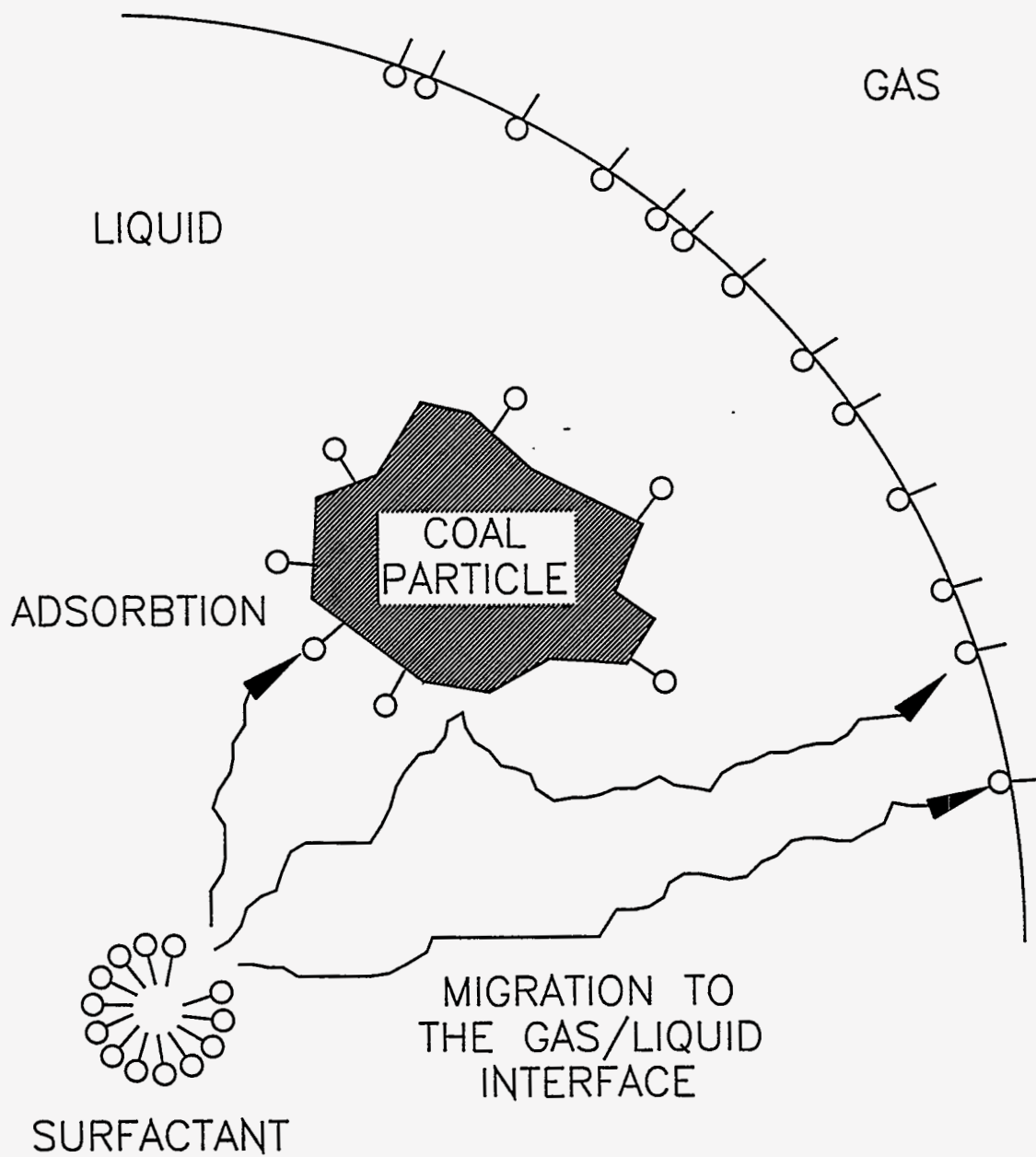


Fig. 3.4 Schematic illustration of adsorption of surfactant at coal surfaces and physical blocking of surfactant migration by coal particles.

0.1% so that the dynamic surface tension behavior can be pronounced, providing the static surface tension level is saturated.

3.3 Dynamic CWS Surface Tension

3.3.1 Maximum bubble pressure technique

Figure 3.5 illustrates the operating principle of the maximum bubble pressure tensiometer technique for dynamic surface tension measurement (Kihm, 1994). The CWS sample is contained in a vessel into which we inserted a specially designed capillary tube with a small outlet diameter of one millimeter. As bubbles formed, grew, and detached from the capillary tube orifice, variations of the bubble pressure occurred because of the change in the bubble radius. Maximum pressure was recorded for each bubble when the bubble radius reached its minimum at the orifice radius. The dynamic surface tension for different bubble generation frequencies was calculated from the measured maximum bubble pressure substituted into a simple relation

$$s = (p_{\max} - \rho gh) r_c / 2 \quad (1)$$

where ρ is the sample fluid (CWS) density, g is the gravitational acceleration, h is the height above the capillary outlet, and r_c is the radius of the capillary outlet. The maximum bubble pressure, p_{\max} , corresponds to the inside air pressure when the radius of the growing bubble equals the capillary radius, r_c . The KRUSS Model BP1 tensiometer was adopted to measure the dynamic surface tension of CWS fuels. The accuracy of the tensiometer was tested by measuring surface tension for distilled and deionized water. The result ensured a satisfactory measurement accuracy showing less than 2% deviations from the surface tension values listed in the CRC Handbook.

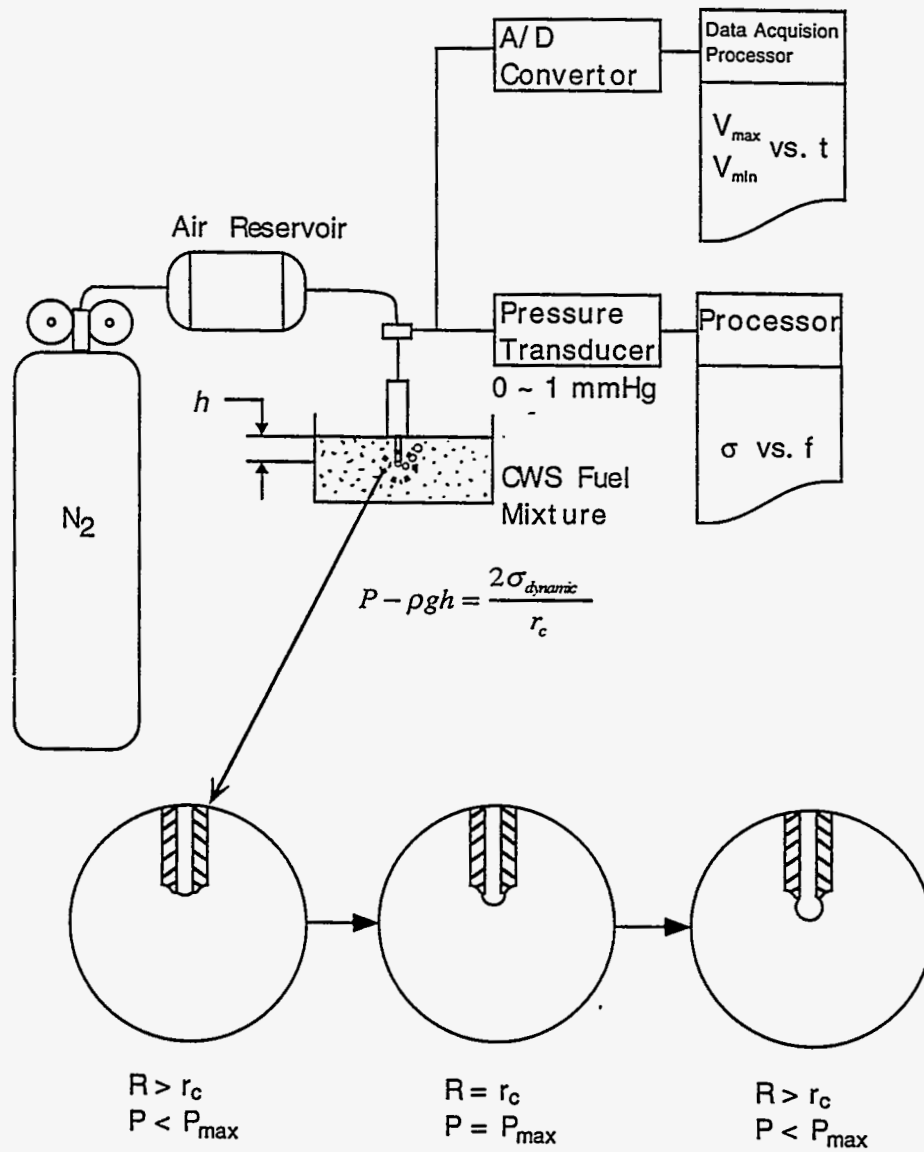


Fig. 3.5 Schematic illustration of maximum bubble pressure tensiometer technique.

3.3.2 Modification of the Kruss tensiometer

The schematic illustration in Fig. 3.1 shows that the analog signal output from the diaphragm type pressure transducer of the Kruss tensiometer is interfaced with an A-to-D board installed in 386 PC. ATLAB data acquisition software from Data Translation Co. samples the analog signals at a rate of 0.2 kHz and digitizes them into the computer memory. A simple FORTRAN program identifies the peak voltage, minimum voltage, bubble life time, and dead time.

Figure 3.6 shows a temporal history of voltage readings for a 1% DDBS-soft aqueous solution. One cycle period of the curve is equivalent to the bubble life time, or the inverse of the bubble frequency. The bubble pressure increases as the nitrogen gas inflow makes the bubble grow, and the bubble diameter decreases from the infinitely large curvature of the initially flat interface at the orifice exit. The bubble pressure increases as the bubble diameter decreases with time. The bubble pressure increases at a faster rate when a surfactant acts to reduce the surface "holding" tension. While the bubble pressure increases, the surfactant migrates to the newly created bubble surfaces. The surface is 'aged' with surfactant diffusion during the period of the ascending curve, which is now called 'diffusion time'. The bubble pressure reaches its maximum value (peak voltage) when the bubble grows to the orifice diameter.

Any further growth of the bubble beyond the peak voltage increases the bubble diameter which, at first, the bubble pressure decreases smoothly. The descending pressure curve then becomes irregular. This is most probably because of the geometrical distortion of the enlarged bubble. The enlarged and distorted bubble detaches from the orifice and the cycle is completed at the time of the minimum voltage reading. The duration from the peak until cycle completion

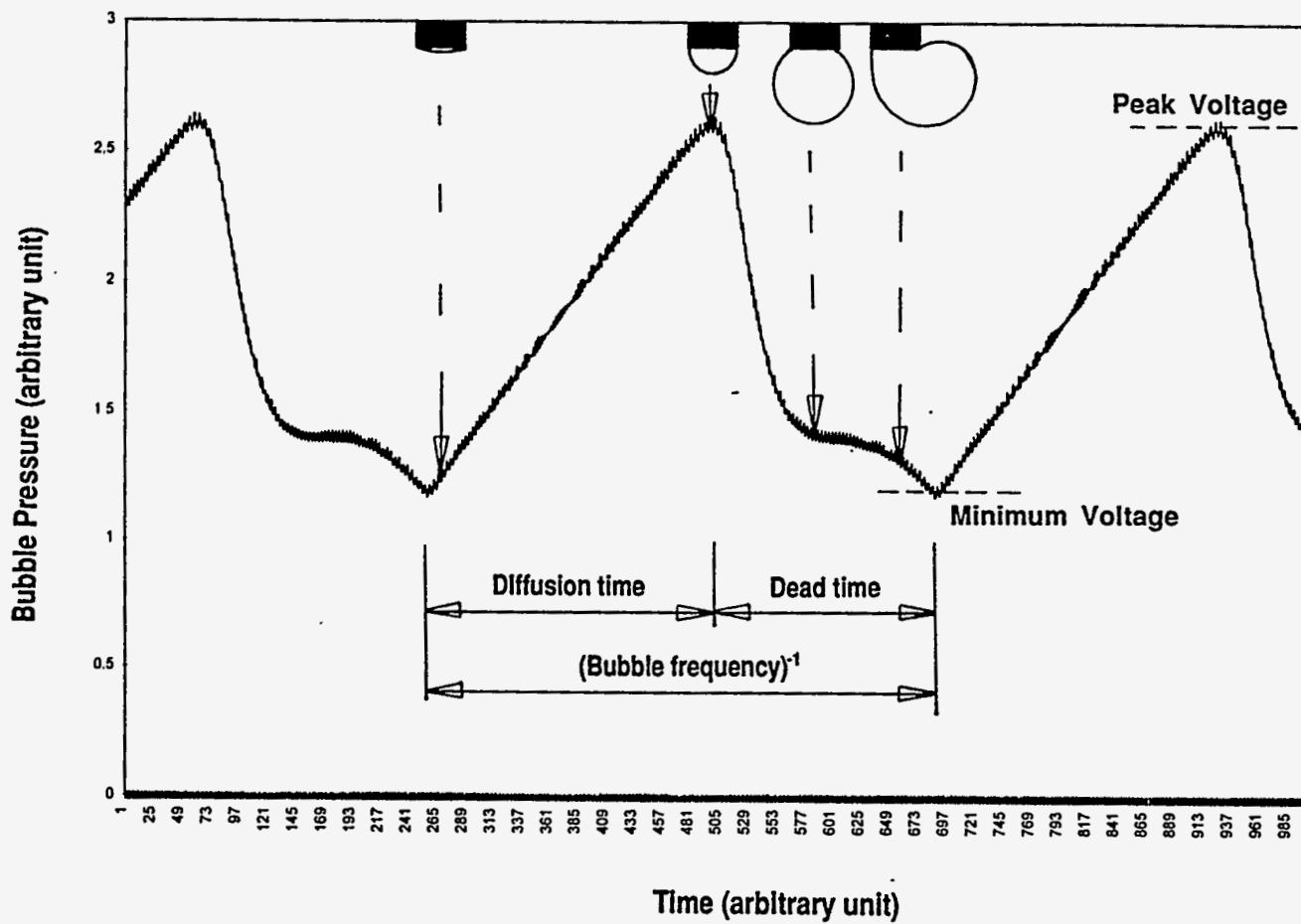


Fig. 3.6 Temporal history of the bubble pressure.

does not directly influence the measurement of the maximum bubble pressure. This time period is now called 'dead time.'

3.3.3 Detailed digitized output reading data

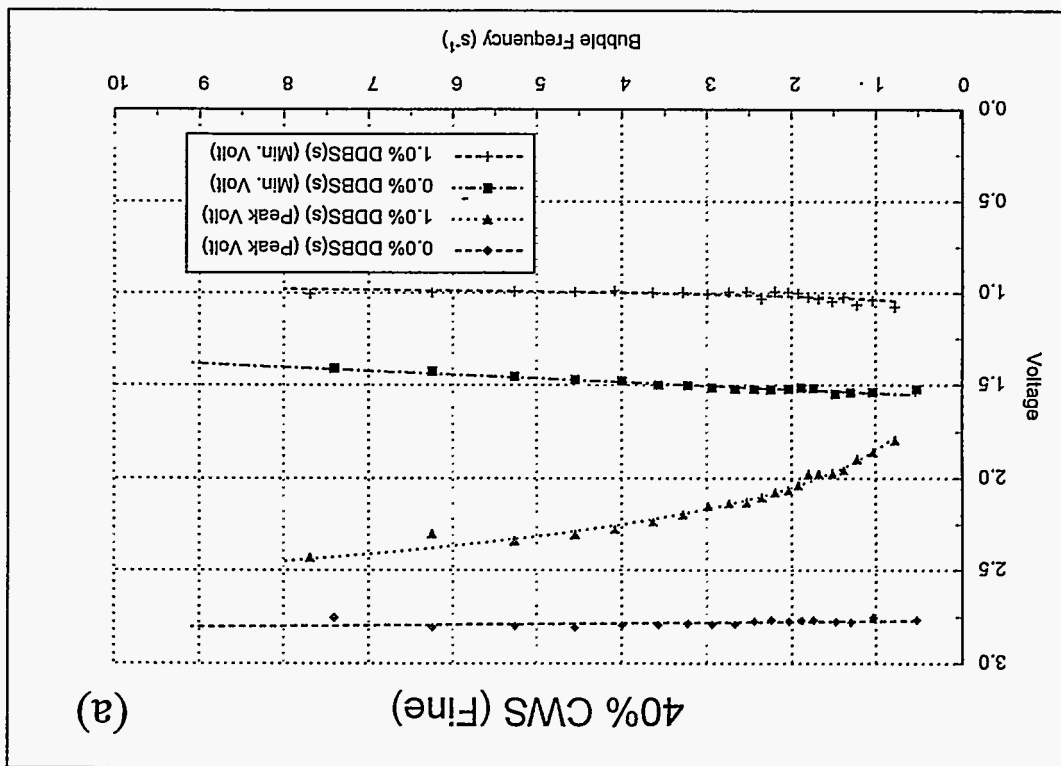
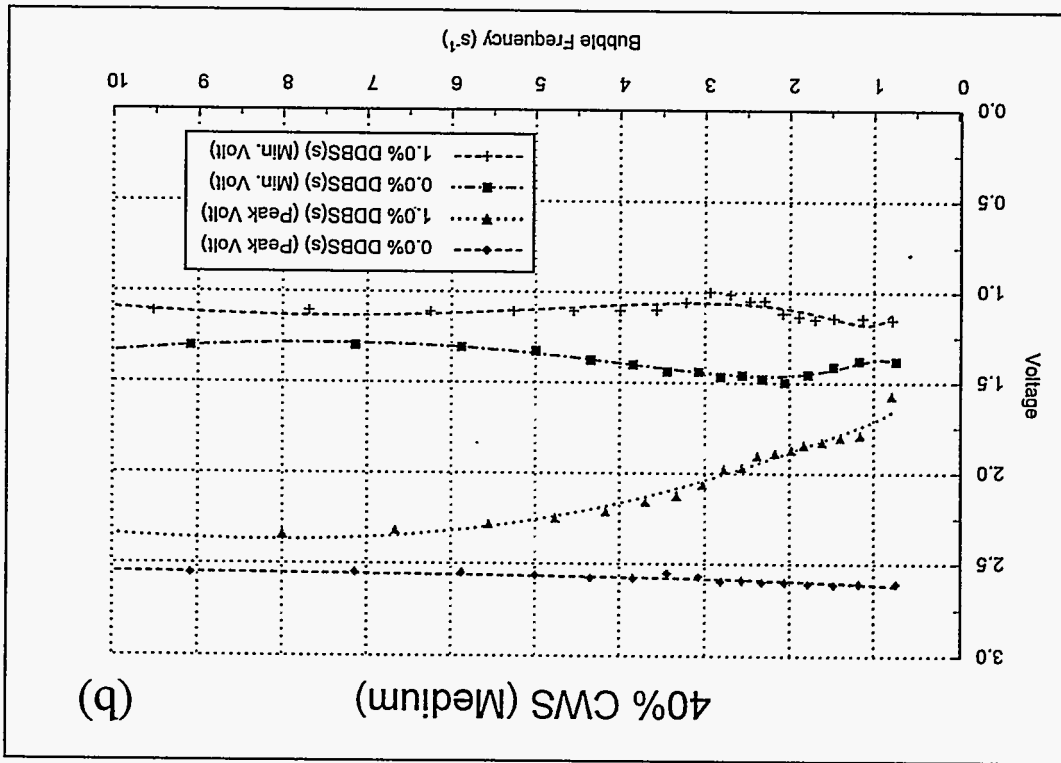
Peak Voltage and Minimum Voltage

Figures 3.7 and 3.8 show the peak and minimum voltage readings versus the bubble frequency for the two CWS samples containing DDBS-soft and 1840-x, respectively. The voltage differential between the peak and the minimum determines the dynamic surface tension values. The higher voltage differentials of the fine samples (Figs. 3.7-a and 3.8-a) compared with the coarse samples (Figs. 3.7-b and 3.8-b) show that the CWS dynamic surface tension tends to decrease with increasing coal particle sizes. This finding is consistent whether the surfactant is present (1.0%) or not (0%). When the surfactant is present, the gradually increasing voltage differential with the bubble frequency shows that the dynamic surface tension increases with the bubble frequency.

The nearly constant minimum voltage over the range of bubble frequencies shows that the system recovers to an identical initial condition before the beginning of the next cycle, and ensures the measurement accuracy for all bubble frequencies. The minimum voltage for the coarse sample shows a slight variation with the bubble frequency. This variation is believed to be because of the bubble pressure detection uncertainties associated with the presence and movement of relatively large coal particles at the gas-liquid interface.

The minimum voltage represents the hydrostatic pressure at the depth of the interface at the time of cycle completion or of new cycle initiation. The minimum voltage can decrease when the gas-liquid interface recedes from the orifice exit and stays inside the orifice at the time of cycle completion. The receding of the gas-liquid interface is likely to occur at higher surfactant

Fig. 3.7 Peak and minimum voltages versus bubble frequency for 40% CWS containing DBS-soft surfactant: (a) fine sample containing coal particles less than 63 μm ; and (b) medium sample containing particles ranging from 180 μm to 250 μm .



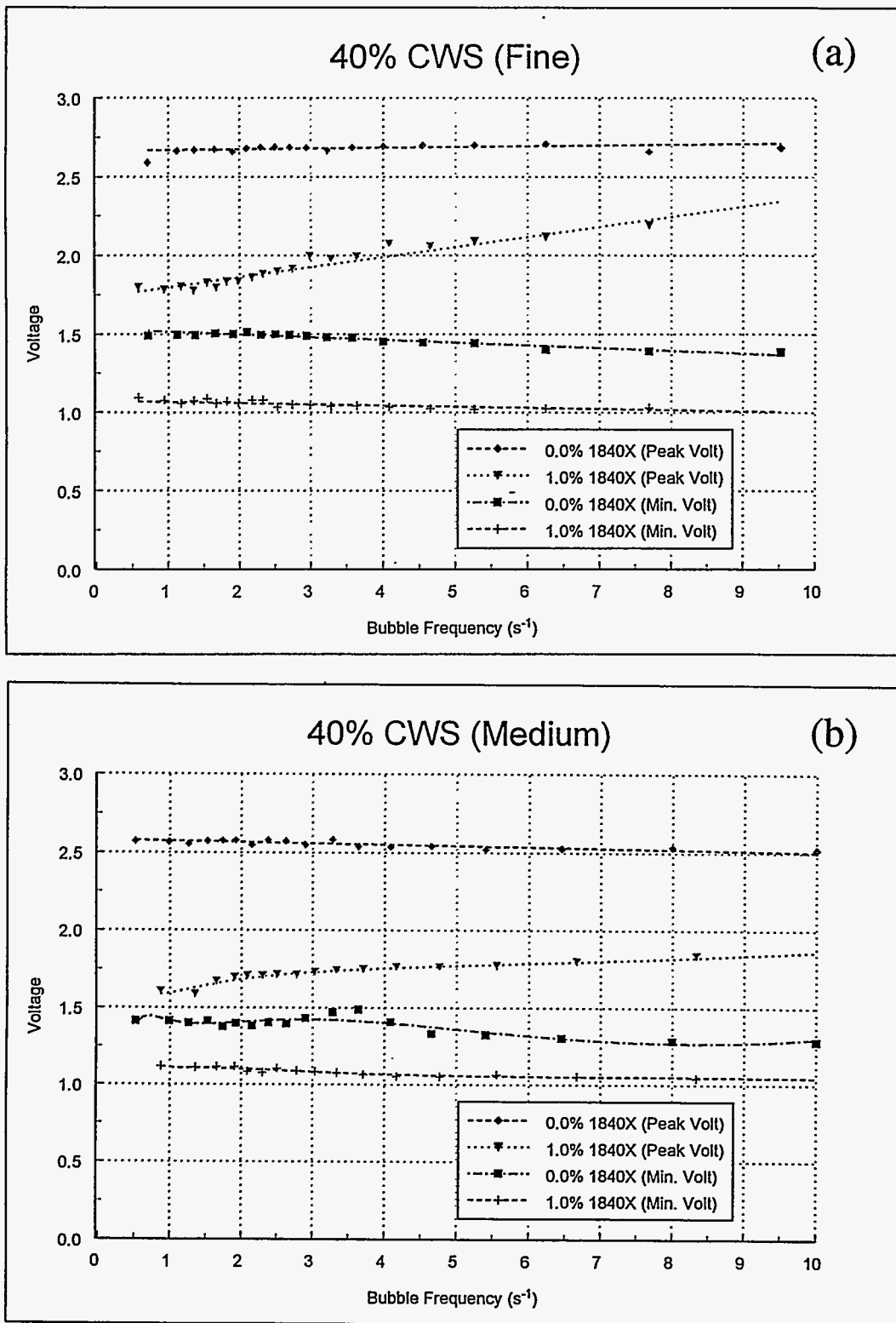


Fig. 3.8 Peak and minimum voltages versus bubble frequency for 40% CWS containing 1840-x surfactant: (a) fine sample containing coal particles less than 63 μm ; and (b) medium sample containing particles ranging from 180 μm to 250 μm .

concentrations that enhance the solution wetting and increases the interface penetration inside the orifice. Results for both fine and coarse samples (Figs. 3.7 and 3.8) show that the minimum voltage level decreases with increasing surfactant concentration.

Increases in the minimum voltage could occur when the hydrostatic pressure is higher than that at the orifice exit. This may occur as a result of an incomplete bubble detachment at the end of the cycle. The remaining undetached portion of the bubble can result in a deeper initial depth than the orifice exit, and the pressure transducer will detect a higher than normal hydrostatic pressure. This type of bias may occur at extremely high bubble frequencies where the dead time is insufficient for full recovery of the cycle with a complete bubble detachment.

Dead Time

Figures 3.9 and 3.10 show the percent of dead time over the bubble life time versus the bubble frequency for the for the two selected surfactants, respectively. The percent of dead time increases linearly with increasing bubble frequency and also increases with increasing surfactant concentration from 0 to 1%. Reduced surface tension at higher surfactant concentrations expedites the bubble growth rate and shortens the diffusion time. The dead time, which occupies the remainder of the bubble life time, increases and its percentage goes up with an increasing surfactant concentration for a given bubble life time.

For a fixed surfactant concentration the dead time ratio increases with the bubble frequency. This implies that the percent of diffusion time decreases with an increase in bubble frequencies, and the surface aging by the surfactant migration is insufficiently achieved. This relatively short diffusion time at higher bubble frequencies retards the full benefit of the surfactant. Larger dynamic surface tension values at higher bubble frequencies can be attributed to the shortened diffusion time with increasing bubble frequency.

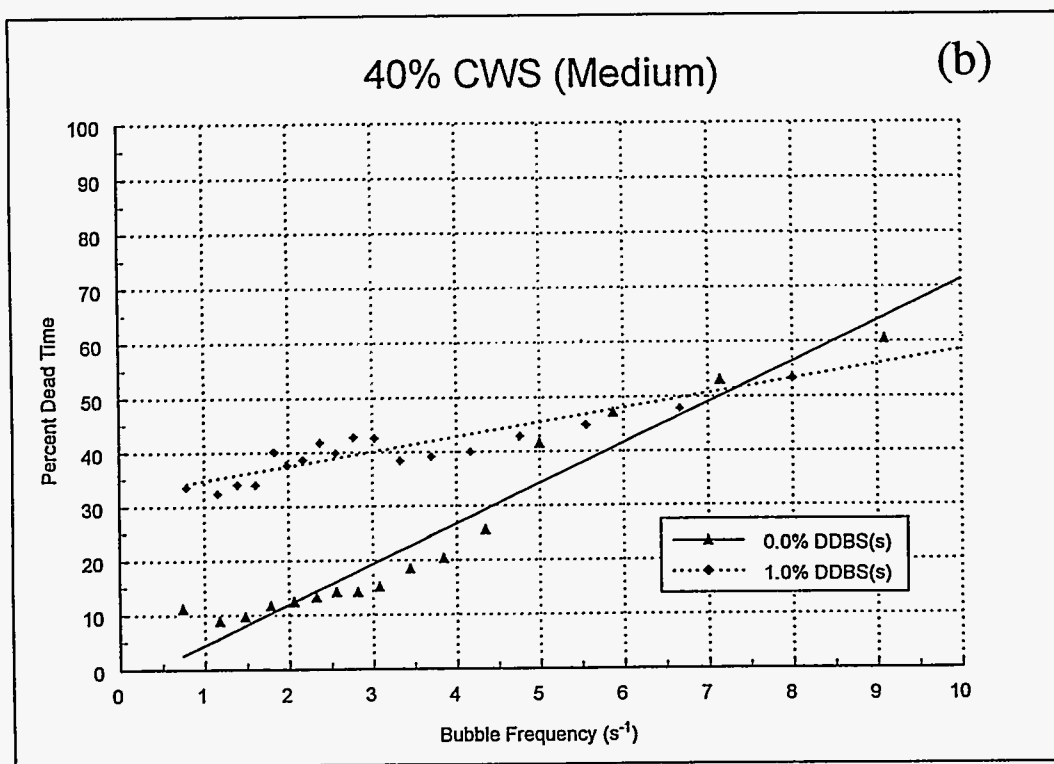
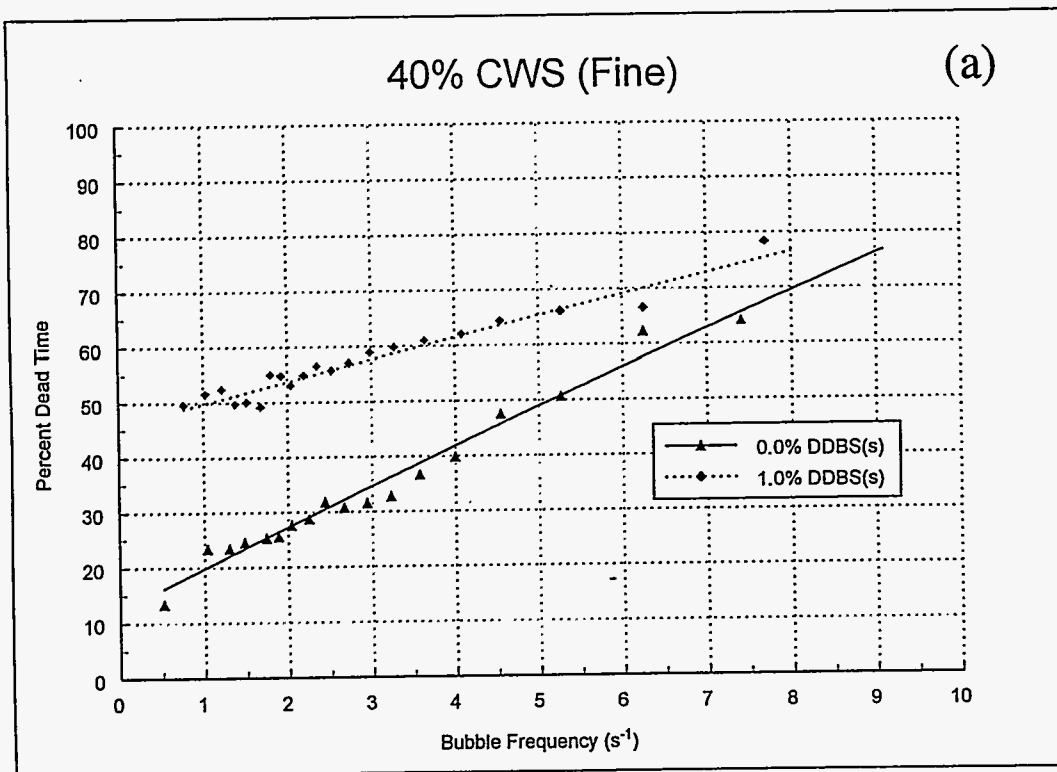


Fig. 3.9 Percent dead time over the bubble life time versus bubble frequency for 40% CWS containing DDBS-soft surfactant: (a) fine sample containing coal particles less than $63 \mu\text{m}$; and (b) medium sample containing particles ranging from $180 \mu\text{m}$ to $250 \mu\text{m}$.

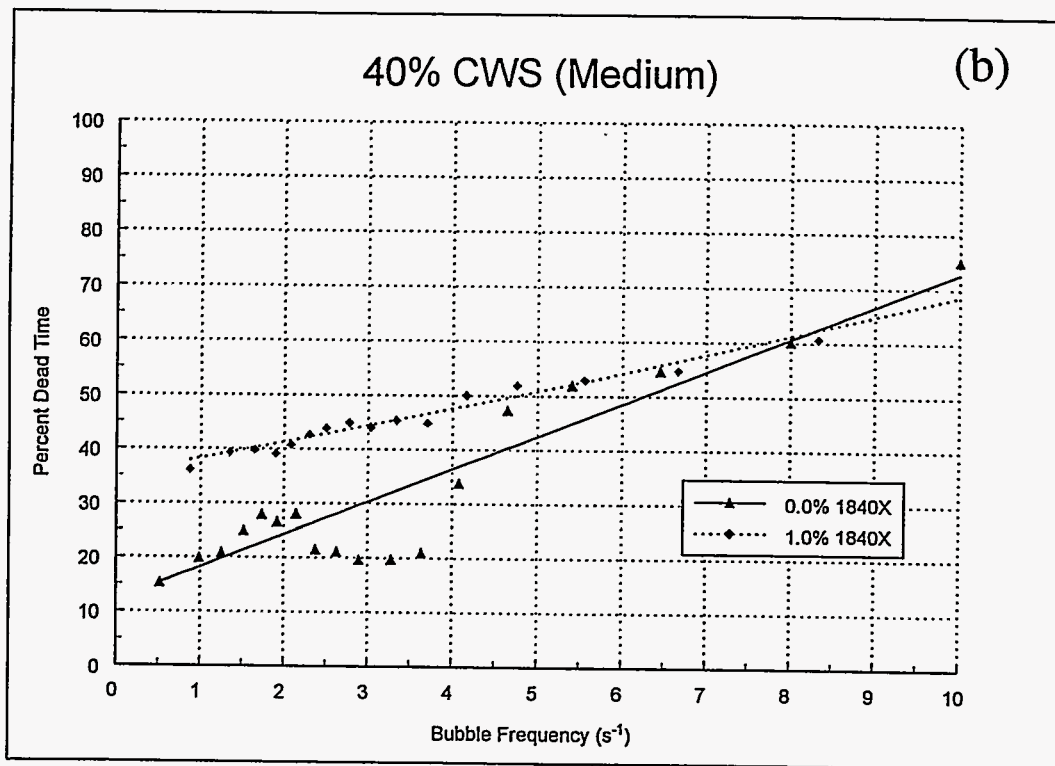
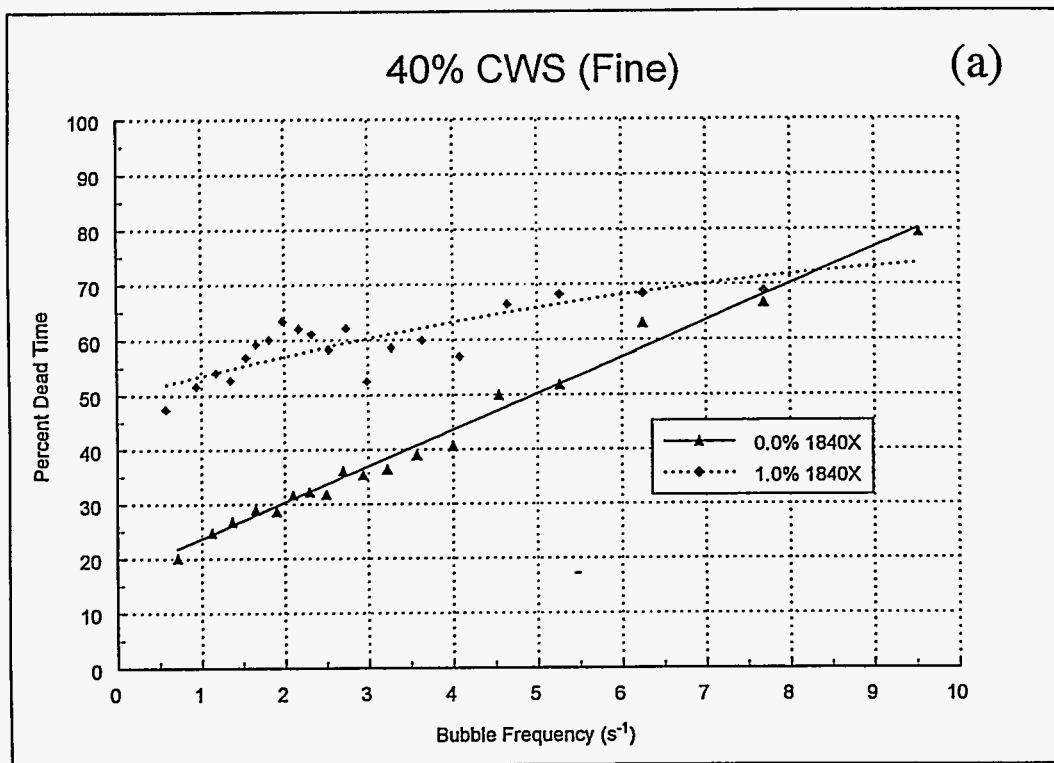


Fig. 3.10 Percent dead time over the bubble life time versus bubble frequency for 40% CWS containing 1840-x surfactant: (a) fine sample containing coal particles less than $63 \mu\text{m}$; and (b) medium sample containing particles ranging from $180 \mu\text{m}$ to $250 \mu\text{m}$.

3.4 Effect of coal particle size on CWS dynamic surface tension

Figures 3.11 and 3.12 show dynamic surface tension data versus bubble frequency for the two selected 40% CWS samples containing DDBS-soft and 1840-x, respectively. Each presents the fine and coarse sample results. The family of curves in each plot, from the top to the bottom, corresponds to 0, 0.1%, 0.5%, and 1.0% surfactant concentrations. At each surfactant concentration, the fine CWS fuel shows consistently higher dynamic surface tension values than the coarse CWS under the same bubble frequency. Three primary reasons for this are: (1) the smaller curvature of radii of fine coal particles enhance the capillary pressure and increases the contact bonding of water between them, (2) smaller coal particles of a higher number density contained in the fine CWS sample enhance the physical blockings against the surfactant migration to the bubble created surface and reduce the surfactant diffusion into the bubble surface (Fig. 4), and (3) the increased total particle surface areas of the fine CWS sample increase the surfactant adsorption.

When the surfactant concentrations are zero or close to the static CMC level of 0.1%, the dynamic surface tension is nearly independent of the bubble frequency, which shows that the dynamic effect on surface tension is not pronounced for low surfactant concentrations. With increasing surfactant concentration, however, the dynamic surface tension shows a gradual increase with increasing bubble frequency, since the increased bubble frequency does not allow sufficient migration time for the surfactant.

3.5 Concluding Remarks

The experimental study using sieve-classified coal particle samples shows that the CWS static and dynamic surface tensions increase with decreasing coal particle sizes under an identical surfactant concentration. The physical reasons are: (1) the larger surface areas of smaller

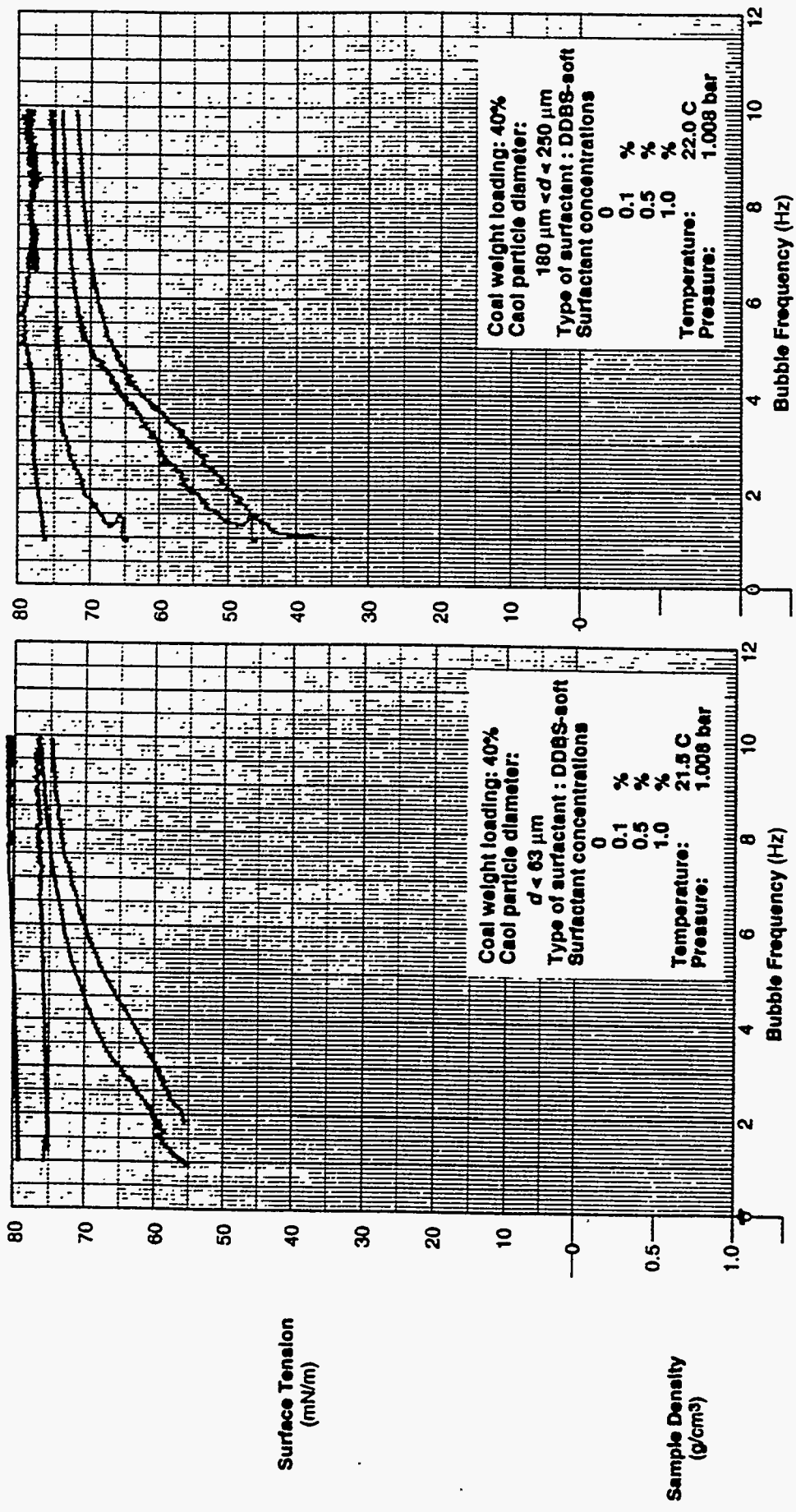


Fig. 3.11 Dynamic surface tension versus bubble frequency for different surfactant concentrations.

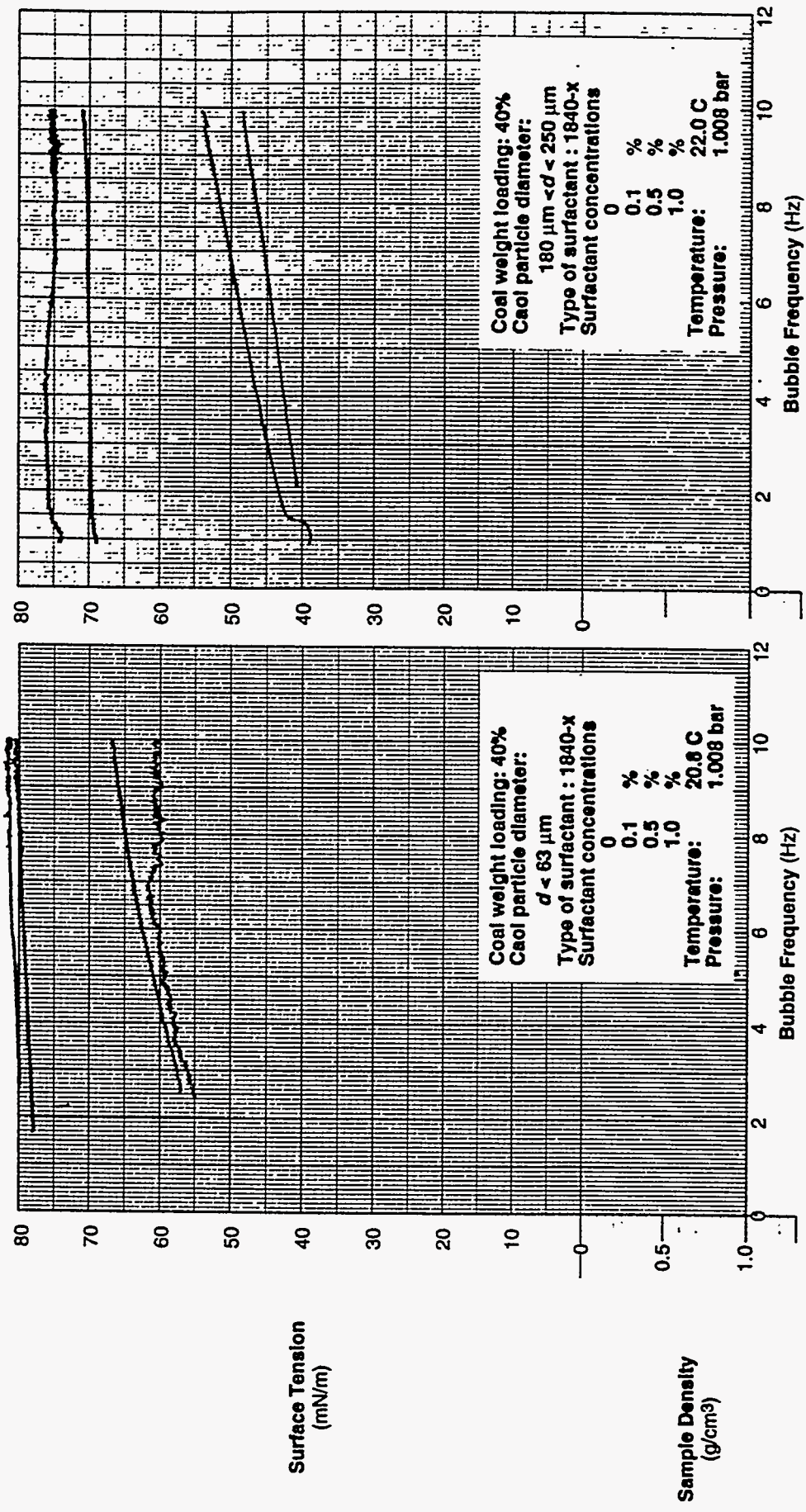


Fig. 3.12 Dynamic surface tension versus bubble frequency for different surfactant concentrations.

particles enhances absorption of surfactant, and (2) the higher number density of smaller particles under the same coal loading increases blocking of surfactant migration to surface.

Chapter 4 Effect of Coal Particle Size on CWS Atomization

Experiments were conducted to investigate the effect of particle size on CWS atomization characteristics. Three different coal powder samples of different sizes were obtained through sieving of coal from the Upper Elkhorn Seam. Preliminary droplet size measurements were made with water sprays and CWS spray measurements were made with 40% coal loading. A sonic air blast configuration was designed and constructed to atomize the highly viscous CWS mixture injected perpendicular to the air stream. Spray Sauter mean diameters (SMDs) were measured at different axial and radial locations using a Fraunhofer laser diffraction particle analyzer (the Malvern system). The results show that CWS mixture containing larger coal particles atomizes into finer sprays than one containing smaller coal particles.

4.1 CWS Sample Preparation

We prepared three different coal powder samples in the range of 32 - 45 μm (Fig. 4.1-a), 45 - 63 μm (Fig. 4.1-b), and 63 - 90 μm (Fig. 4.1-c). All the tested CWS samples contain 40% coal loading and 0.5% Flocon as a basic additive. Coal particles larger than 90 μm sediment too fast due to their large gravitational effect, and injection of CWS containing such large particles easily separates them from water. For this reason, the sample particle size was limited to 90 μm . The lower limit of 32 μm was set because the sieved amount of coal particles below 32 μm was too small.

Figures 4.2-a to c are photographs of coal particles after being mixed with water. A sampling was made at the atomizing orifice and the water was dried off from the sampled CWS. The lengthy running of the rotating tumbler while mixing with water generated a significant amount of small sized crumbled particles. This disintegration is more pronounced for the sample containing the largest coal particles (63-90 μm). However, the sample containing the smallest



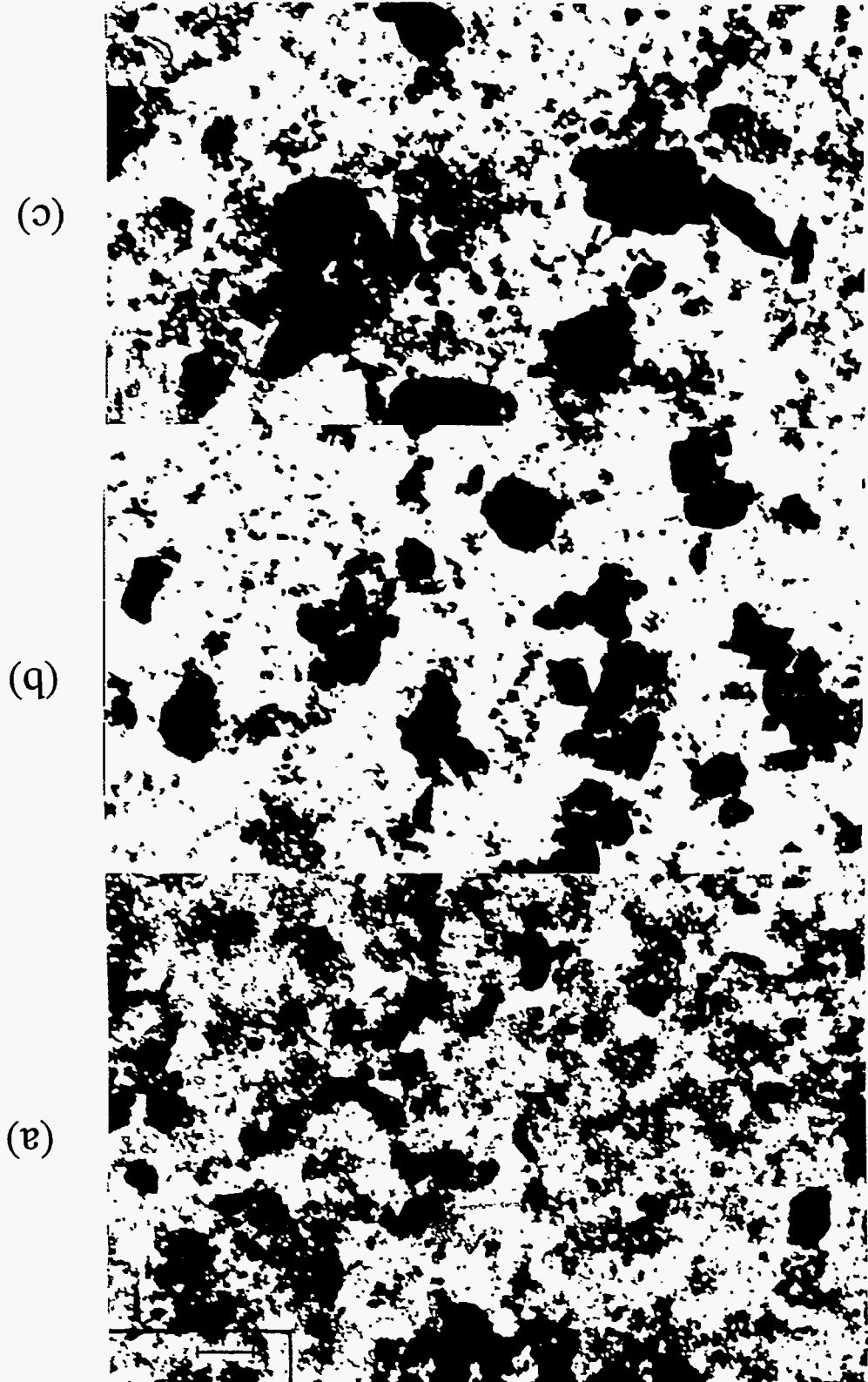
(a)

(b)

(c)

Fig. 4.1 Size classified coal particles sampled as powder.

Fig. 4.2 Size classified coal particles sampled as CWS.

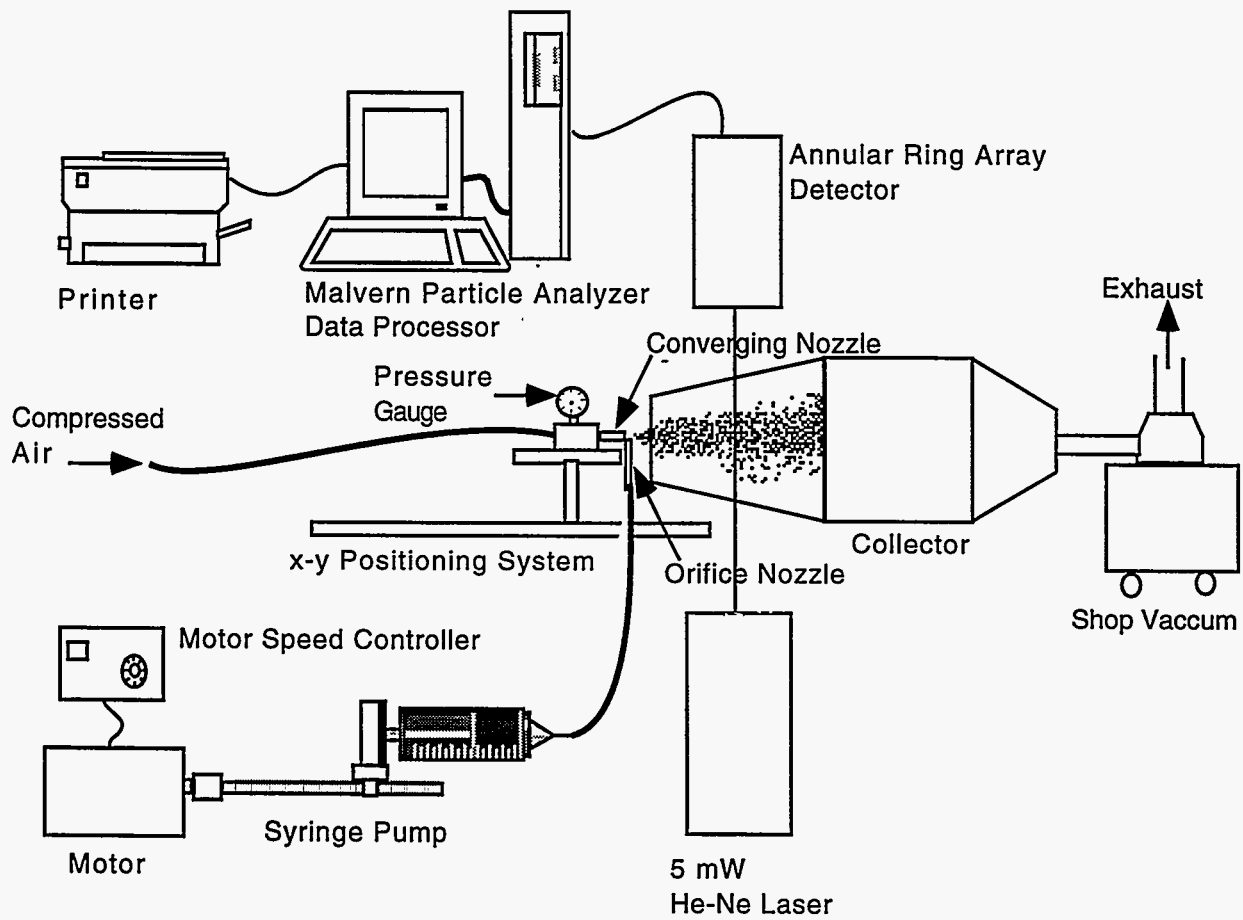


particles (32-45 μm) is nearly unchanged since they are already as small as the crumbled particles. Despite the disintegration of larger particles in CWS mixing, the three samples are clearly distinguishable by their representative particle size ranges, which generally compare to the original samples shown in Figs. 4.1-a to c.

4.2 Experimental Setup for Sonic Airblast Atomization

Figure 4.3 shows a schematic illustration of a sonic atomization system specifically designed and constructed to efficiently atomize highly viscous CWS mixtures. A compressed air jet exhausts from a converging nozzle to provide high shear energy for atomizing the cross-injected CWS mixture. A positive displacement syringe pumps the CWS mixture, and operates by a stepper motor connected to a speed controller to ensure a constant injection rate. The Malvern diffraction particle analyzer measures spray SMDs assuming Rosin-Rammler two-parameter distribution (Rosin and Rammler, 1933).

The converging nozzle establishes a sonic exit flow when the stagnation pressure reaches 191.7 kPa (13.1 psig) for one atmospheric back pressure of 101.3 kPa (0 psig or 14.7 psia). This condition is called a perfect or isentropic expansion. When the stagnation pressure exceeds 191.7 kPa, the jet Mach number remains at unity but the jet exit condition becomes an underexpanded state exhausting increased air mass flow rate. The underexpanded air must expand outside the nozzle by way of Prandtl-Meyer expansion fans. The air mass flow rate increases linearly proportional to the stagnation pressure. This increased mass flow rate of the underexpanded sonic jet provides higher air blast shear energy and finer atomization with smaller SMDs.



4.3. Experimental setup of sonic airblast atomization system.

4.3 Preliminary Measurements Using Aqueous Solutions

Figure 4.4 shows the preliminary results of SMD variations for water sprays under three different underexpanded air jets at 20, 40, and 56 psig (2.39, 3.77, and 4.87 bars in absolute, respectively). The measurements were conducted along the spray center ($y = 0$) at different axial locations x/D_{th} , where D_{th} is the air nozzle exit diameter. Spray SMDs first decrease because of the breakup of ligaments and larger drops into smaller drops, and reach a minimum SMD at a certain x -location. The spray SMDs then gradually increase, mainly because of the coalescence between drops as they travel downstream. Preferential evaporation of smaller drops also contributes to increasing the spray SMDs with increasing x . Note that the location of minimum SMDs, x_{min} , remains nearly unchanged as $x_{min} / D_{th} \approx 30$ for different stagnation pressures.

Figure 4.5 shows spray SMDs measured for 100% ethanol whose surface tension is 22.75 dyne/cm at 20 C, approximately 30% of the water surface tension at the same temperature, while the viscosity of ethanol remains nearly identical to that of water. The significantly lower surface tension of ethanol is attributed to the smaller SMDs by a factor of one-half or less than the water spray SMDs. The lower surface tension develops sprays more readily and results in smaller $x_{min} / D_{th} \approx 15$ for ethanol sprays.

4.4 Effect of Coal Particle Size on CWS Atomization

Figure 4.6 shows SMDs measured along the spray axis of $y = 0$ at 20 psig air pressure for three CWS samples containing coal particles in different size ranges. The initial decrease of SMDs and then the gradual increase of them are similar to the case of water sprays in Section 4.3. However, the spray SMDs *decrease* with increasing coal particle sizes while the reverse was expected. We have seen that both static and dynamic surface tension properties of CWS samples containing larger coal particles measured smaller when compared with the CWS properties for

Water, Flow rate = 2 ml/s, FD=100mm, y=0

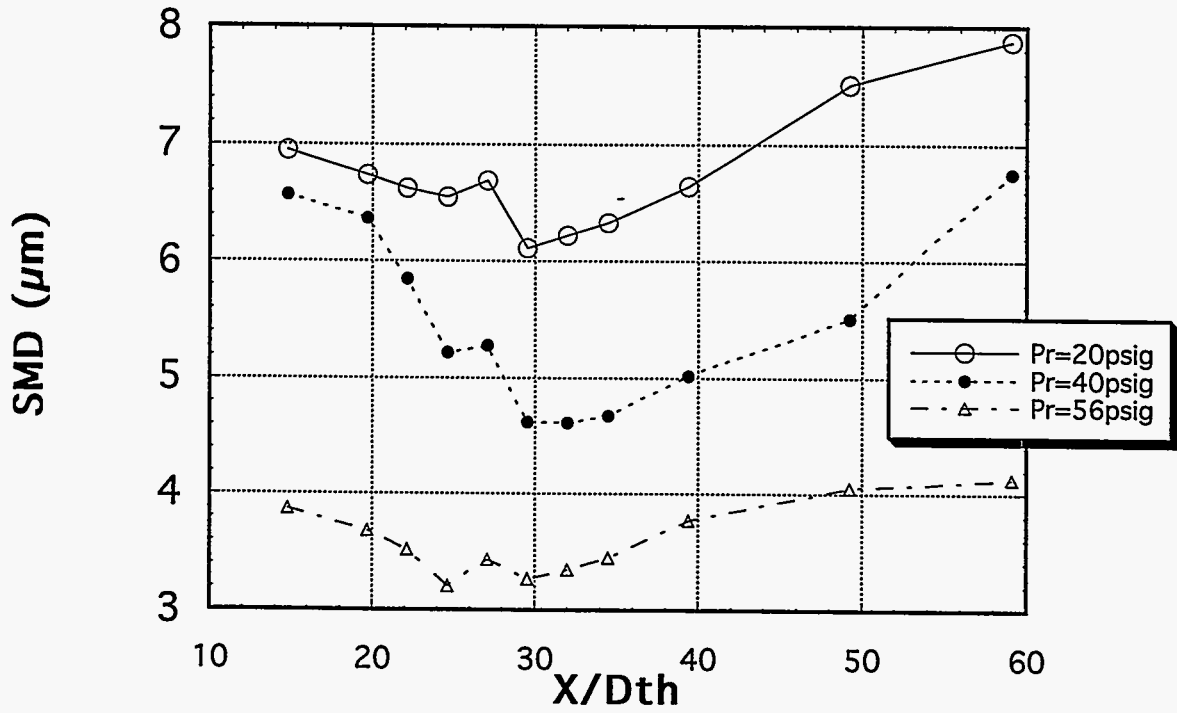


Fig. 4.4 Water spray SMD variations along the jet axis for three different air pressures.

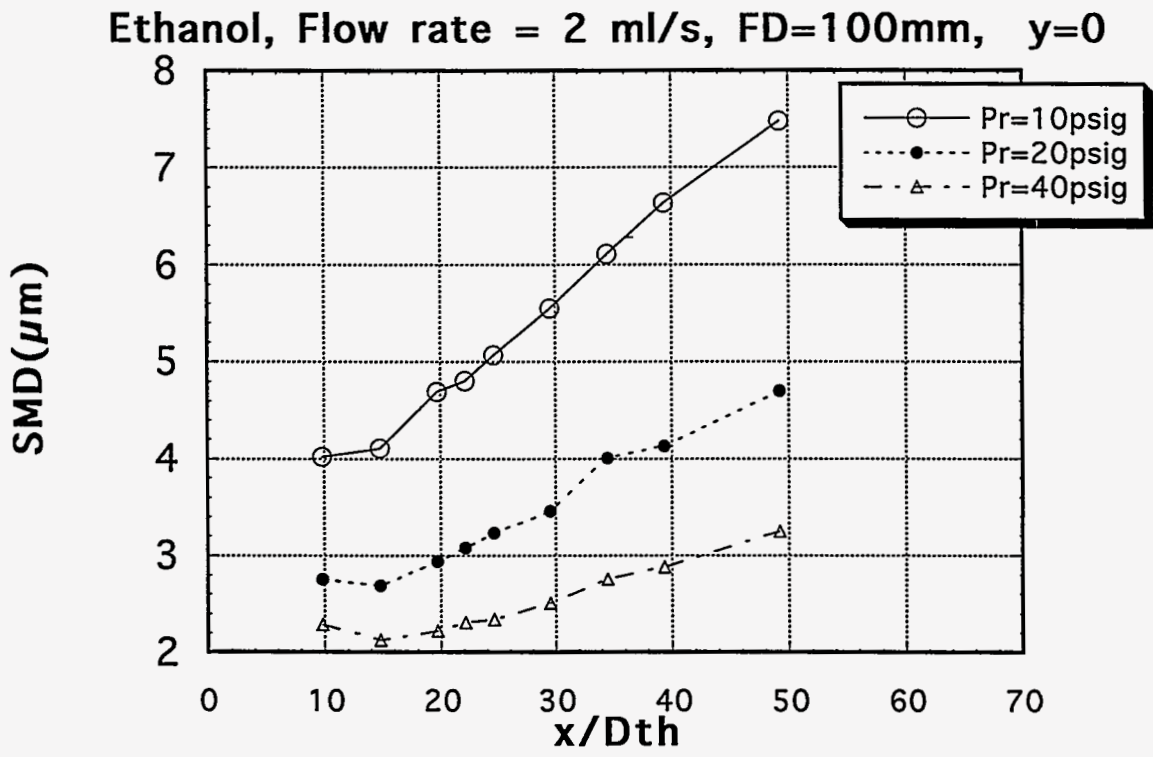


Fig. 4.5 Ethanol spray SMD variations along the jet axis for three different air pressures.

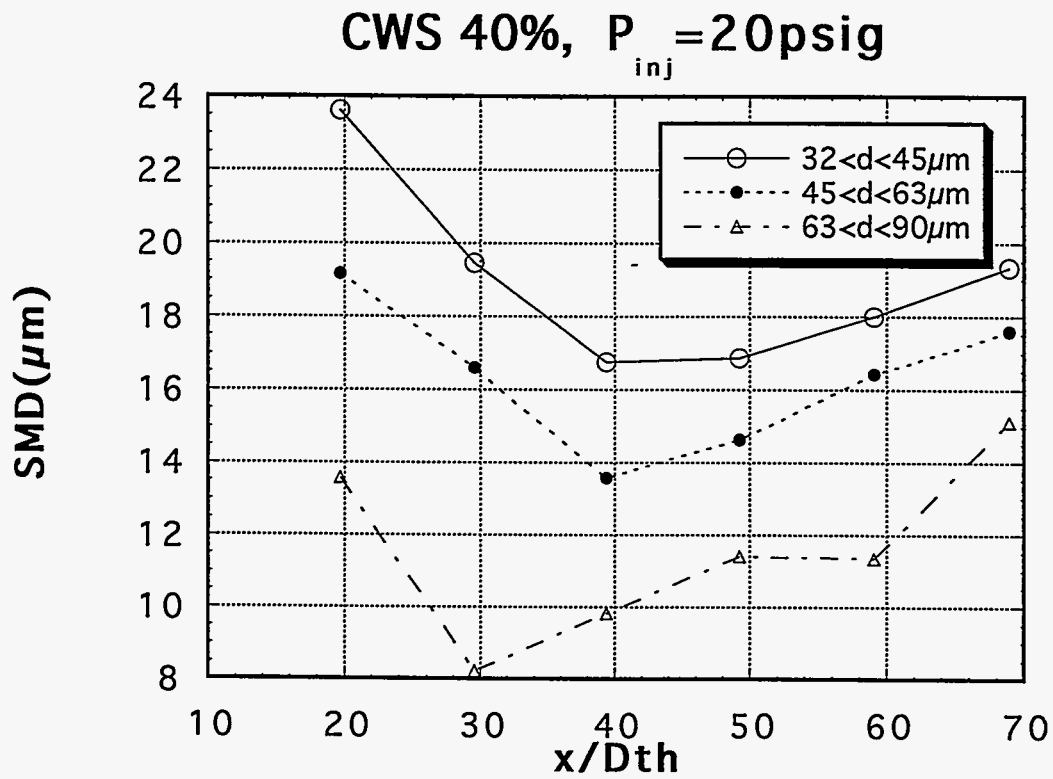


Fig. 4.6 Axial SMD variations of 40% CWS sprays containing differently sized coal particles.

smaller coal particles (see section 3.3.4). Therefore, it is believed that a primary reason for smaller SMDs of CWS containing larger particles is because of its lower surface tension, which helps for easier breakup and finer atomization.

A more physical explanation for the subtle slurry atomization characteristics has been sought, and a highly feasible conjecture is proposed that considers the capillary pressure levels between neighboring particles suspended in water (Fig. 4.7). Upon the injection of the CWS mixture through a small orifice, large drops or ligaments form as a result of the instability growth and these larger drops or ligaments are immediately shattered by the high pressure blasting air jet. The large coal particles retain a relatively weak capillary pressure between them because of their larger radii of curvature. The weak hydration bonding makes large particles separate easily from each other and water can be readily stripped off the coal surface under a strong air blasting jet. Also, the number density of larger particles is low and their coalescence is weaker. As a result, the atomization of the CWS mixture containing large coal particles can take place two-fold: (1) fine sprays of nearly pure water droplets from the water separated from coal particles, and (2) medium sized drops containing only a limited number of coal particles.

On the other hand, the ligaments or drops containing small coal particles carry a higher particle number density whose total surface areas will also be larger. The small particle dimension ensures stronger capillary bonding between particles and the coalescence between them will be strong. When exposed to the air jet, the water will not be easily stripped off because of the strong hydration bonding, and the strong coalescence between particles will generate relatively good-sized droplets that contain a number of small coal particles strongly bonded inside. This can explain why CWS containing smaller particles atomizes into relatively larger droplets.

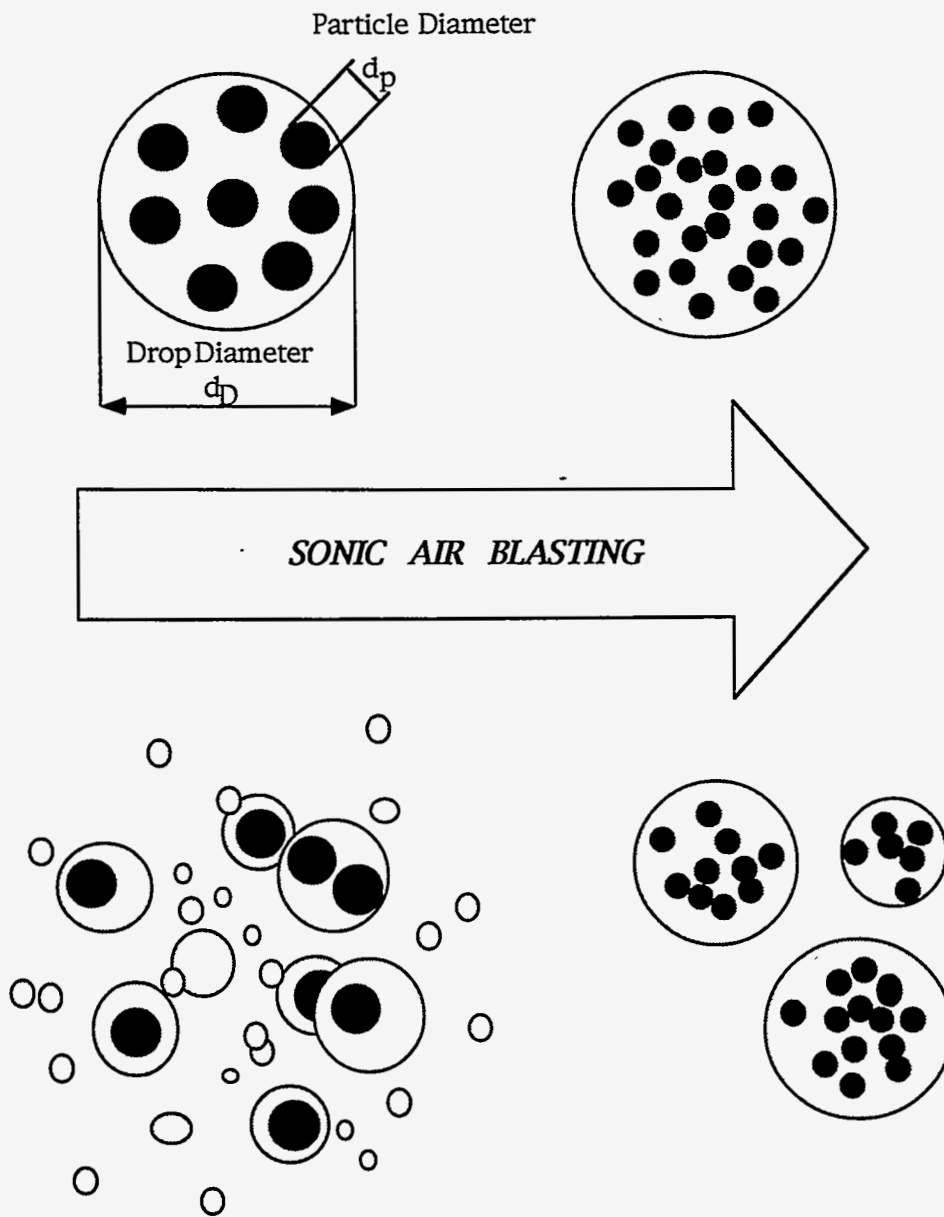


Fig. 4.7 Schematic illustrations of airblast breakup of two different slurry ligaments containing coal particles of different sizes.

Figure 4.8 presents evidence to support the conjecture discussed above. Drop diameter spectra in volume percentage are shown for three CWS sprays and water spray at the location of minimum CWS spray SMDs, i.e., $x_{\min} / D_{th} \approx 40$. With an increase in coal particle sizes, the peak shifts to a smaller diameter and the spray SMD decreases. At the same time, the drop diameter spectrum of CWS spray containing larger coal particles approaches that of the water spray. This explains why the water held between large coal particles is easily separated from them, and the resulting spray contains a significant portion of nearly pure water spray. For CWS containing smaller particles, the spray drop size spectrum deviates away from the pure water spectrum since the water stripping is not very plausible.

Figures 4.9 to 4.11 show the CWS spray SMD variation in the y-direction perpendicular to the axis for the three tested samples, respectively. The preferential evaporation of smaller droplets near the spray edge and weaker air blasting shear energy make the spray SMD increase as y increases (or y decreases in the negative direction). For the smallest coal particles (Fig. 4.9), the relatively strong holding of water in CWS competes with the air injection pressure. Large SMDs at 10 psig air pressure show that each drop may contain several coal particles due to the strong capillary holding. The air blasting is not strong enough to overcome the surface tension at the drop surface and the portion of stripped water spray is not noticeable. When the air pressure increases to 40 psig, SMD decreases dramatically as the strong air blast action overrides the surface tension of drops and shatters the capillary holding between particles.

The dependence of the SMD spectrum on the air pressure is reduced for the medium range of coal particles (Fig. 4.10) and the three spectra tend to collapse into a single curve for the largest coal particles (Fig. 4.11). The relatively weaker capillary pressure between the larger particles allows easier water stripping and separation for low to moderate air pressure.

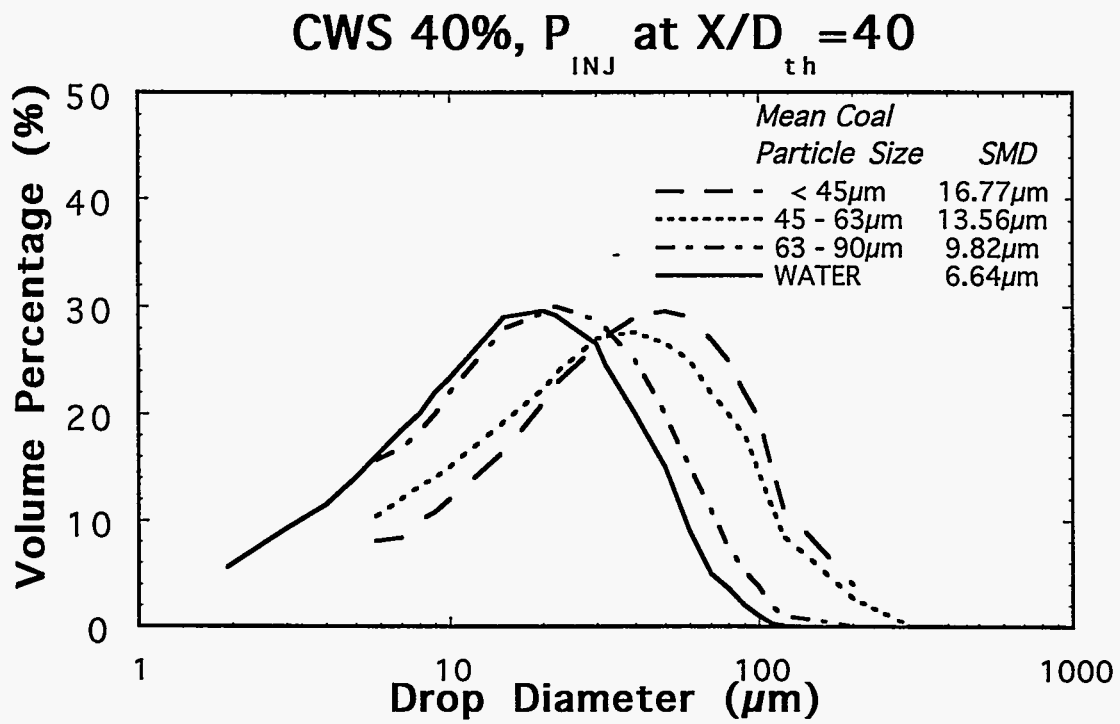


Fig. 4.8 Volumetric percentile spectra of drop diameters of three different 40% CWS sprays and water spray at under 20 psig air pressure.

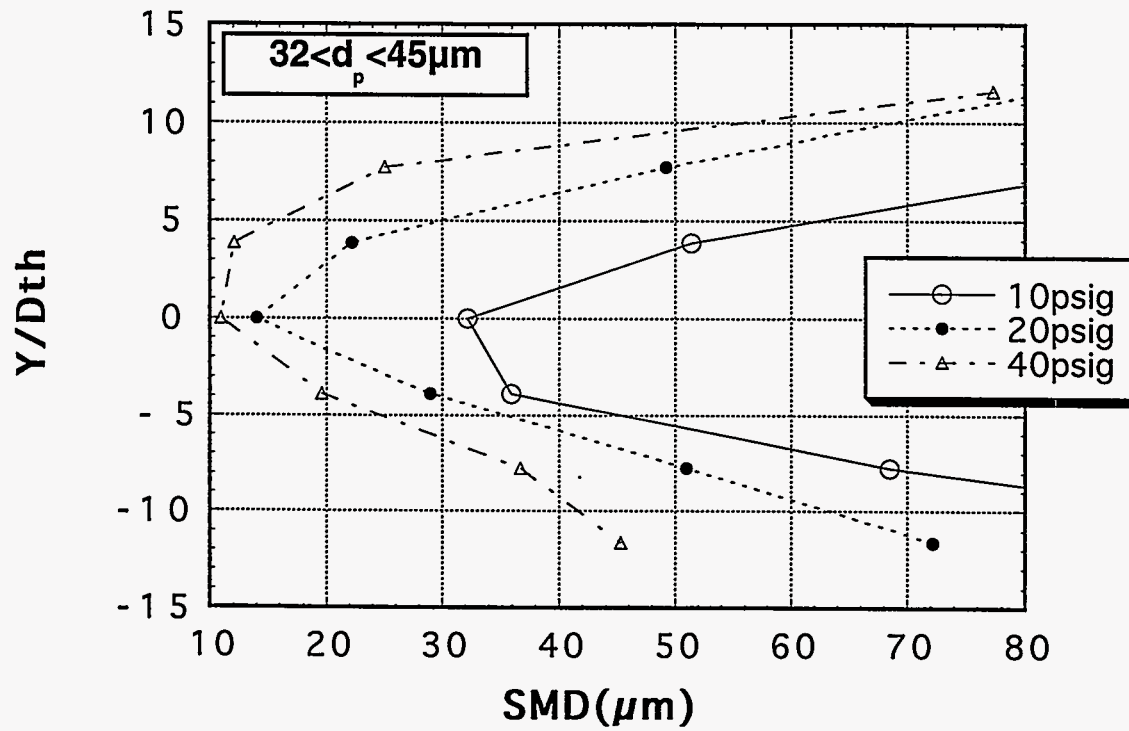


Fig. 4.9 Radial SMD variations of 40% CWS (coal particles in $32 \mu\text{m} < d_p < 45 \mu\text{m}$) sprays measured at $x/D_{th} = 40$ under different air pressures.

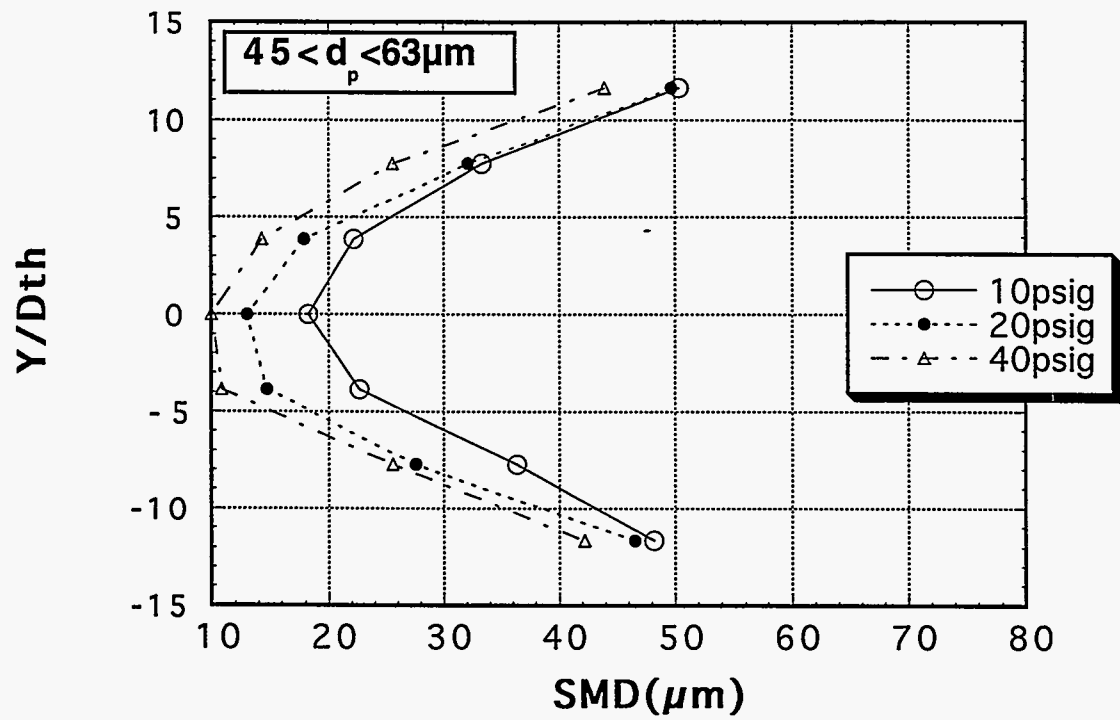


Fig. 4.10 Radial SMD variations of 40% CWS (coal particles in $45 \mu m < d_p < 63 \mu m$) sprays measured at $x/D_{th} = 40$ under different air pressures.

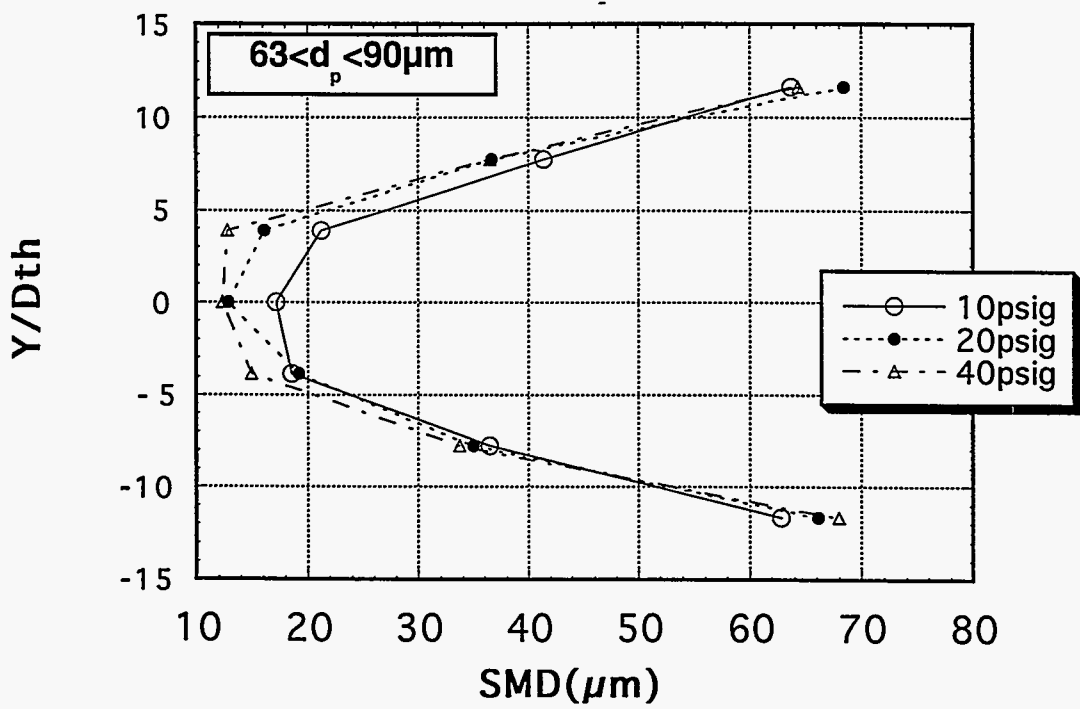


Fig. 4.11 Radial SMD variations of 40% CWS (coal particles in $63 \mu\text{m} < d_p < 90 \mu\text{m}$) sprays measured at $x/D_{th} = 40$ under different air pressures.

The effect of air pressure on the spray SMDs is more comprehensively shown in Figs. 4.12 to 4.15 for the three tested CWS samples. Again, a consistent competition is observed between the airblasting energy (external) the surface tensional (interfacial), and capillary holding energy (internal) for different samples of different particle sizes.

The low airblast at 4 psig (Fig. 4.12) barely strips off water from ligaments containing the largest particles (63-90 μm) and makes its SMD distribution shift toward the smaller water spray SMD level. The other two samples that contain smaller coal particles do not lose water due to their stronger water retention. However, as the air pressure increases, the medium sample shows a yield to the external air blast that results in a noticeable SMD decrease at 10 psig (Fig. 4.13). All three samples are then dominated by the increased air blast at 20 psig (Fig. 4.14). At the higher air pressure of 40 psig, all three curves collapse into a single one where different levels of internal holding and interfacial tensile energies of the three different samples are completely overridden by the extremely strong external air blast energy.

4.5 Concluding Remarks

Experimental investigations show that a CWS containing larger coal particles atomizes into sprays of smaller mean diameter, while a CWS containing smaller coal particles atomizes into sprays of relatively larger mean diameter. The CWS containing large particles loosely hold water because of its weak capillary holding and coal particles easily separate. The resulting spray consists in part of nearly pure water droplets and CWS droplets containing a limited number of coal particles. As a result of the fine water spray, the overall mean drop diameter shows a decrease with increasing coal particle size. On the other hand, smaller coal particles strongly coagulate and their CWS mixture atomizes into moderately sized drops containing many coal particles.

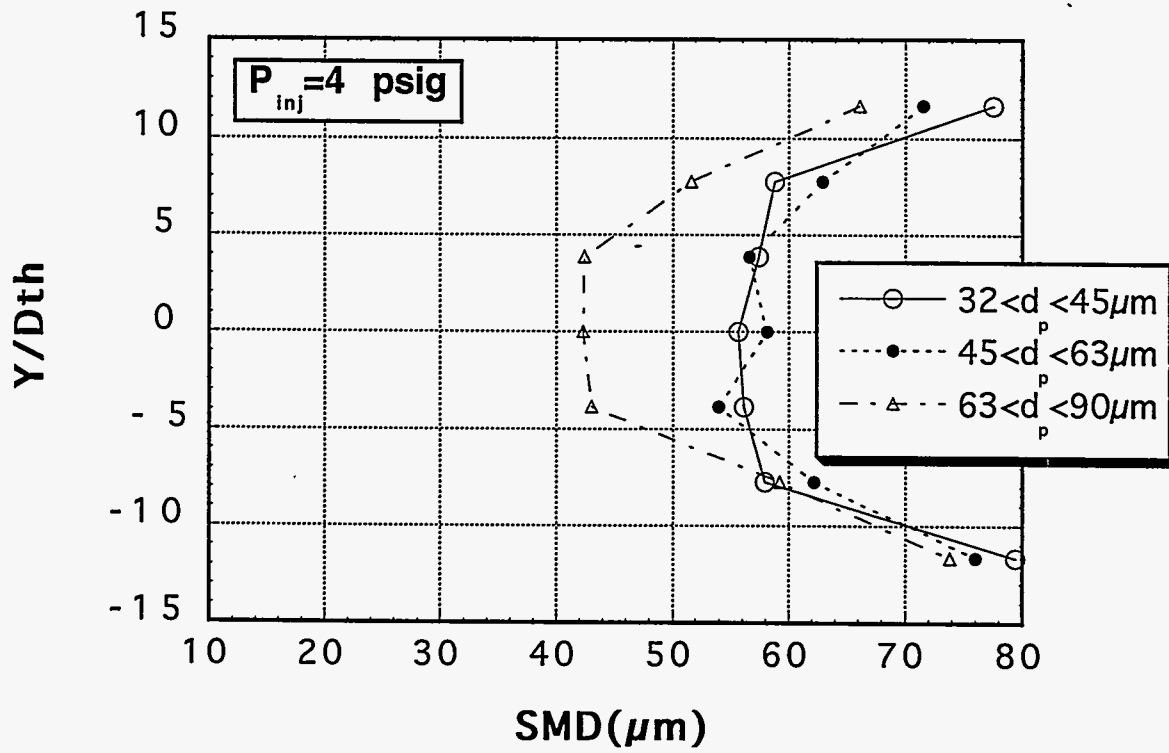


Fig 4.12 Radial SMD variations of 40% CWS sprays containing differently sized coal particles measured at $x/D_{th} = 40$ under 4 psig air pressure.

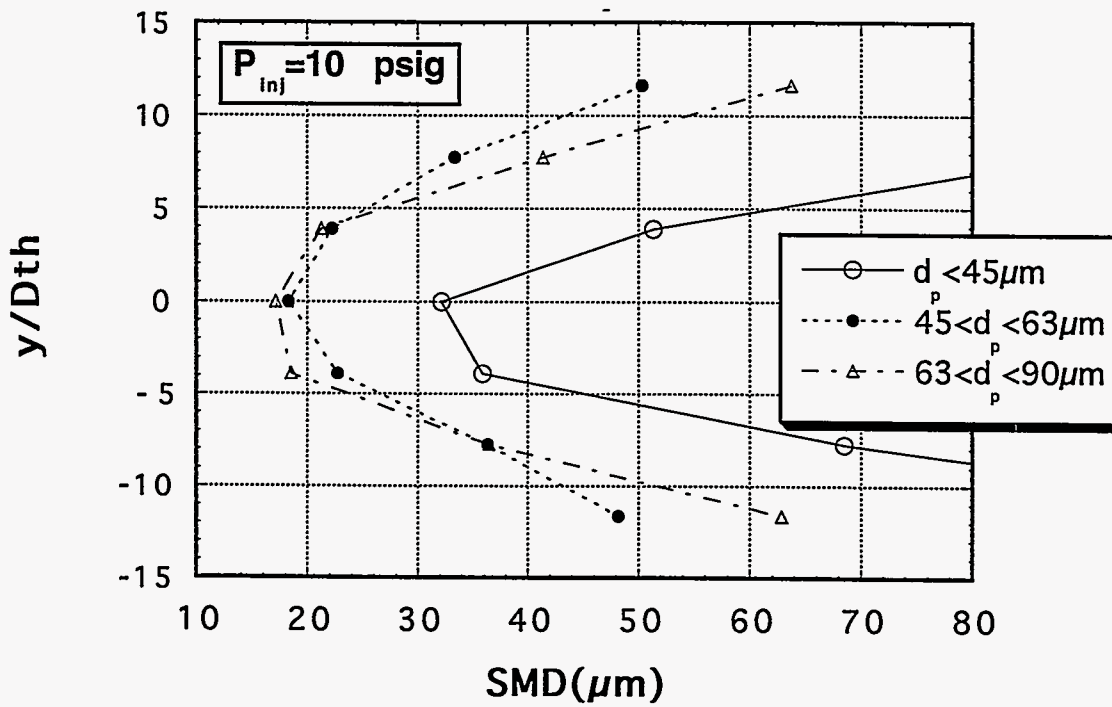


Fig 4.13 Radial SMD variations of 40% CWS sprays containing differently sized coal particles measured at $x/D_{th} = 40$ under 10 psig air pressure.

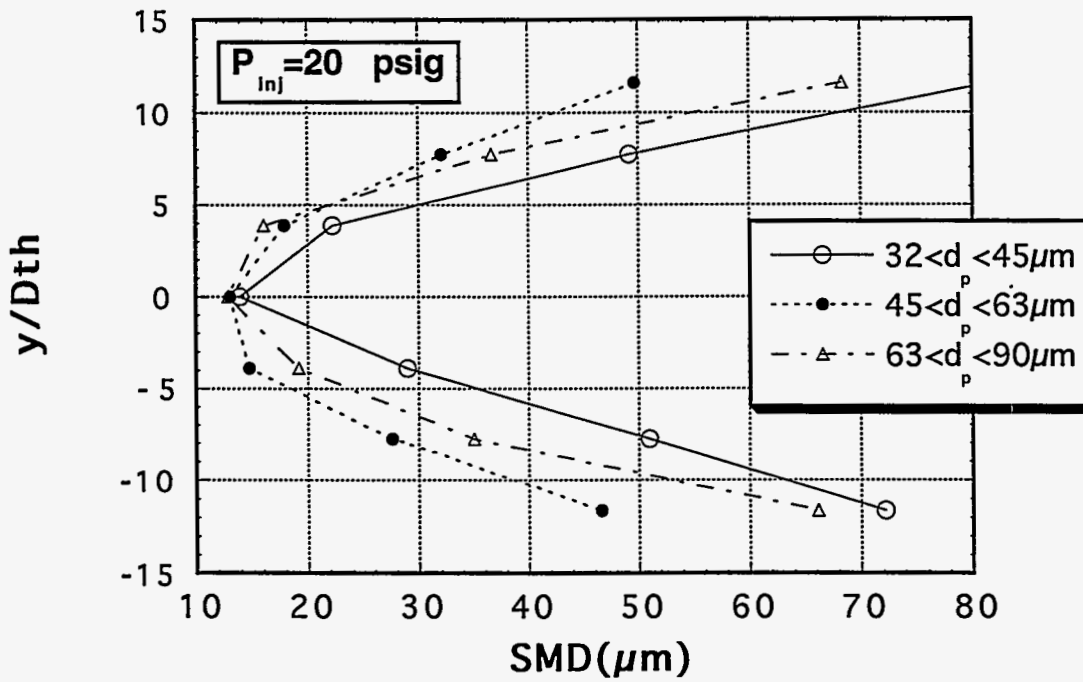


Fig 4.14 Radial SMD variations of 40% CWS sprays containing differently sized coal particles measured at $x/D_{th} = 40$ under 20 psig air pressure.

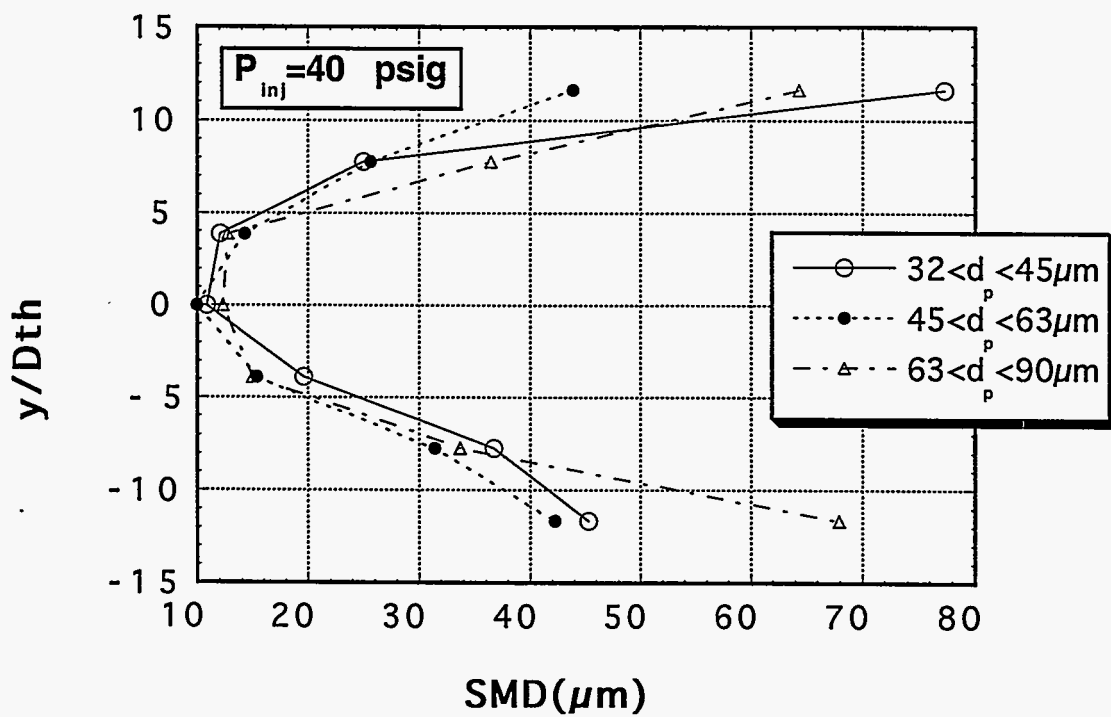


Fig 4.15 Radial SMD variations of 40% CWS sprays containing differently sized coal particles measured at $x/D_{th} = 40$ under 40 psig air pressure.

Chapter 5 Summary and Conclusion

The effects of coal particle size on the CWS interfacial properties was examined by measuring both static and dynamic surface tension for two different CWS samples containing fine and coarse coal particles. The current experimental finding shows that the CWS static and dynamic surface tensions increase with decreasing coal particle sizes. This is attributed to increased surfactant adsorption due to the larger surface areas and increased physical blocking of surfactant migration due to the higher number density of smaller particles under a given coal loading.

Experimental investigation shows that a CWS containing larger coal particles atomizes into sprays of smaller mean diameter, while a CWS containing smaller coal particles atomizes into sprays of relatively larger mean diameter. Based on different experimental evidence it is conjectured that three different energies are competing in slurry atomization: (1) *the internal capillary holding* between particles and water, (2) *the interfacial surface tensile* energy at the slurry surface contacting air, and (3) *the external air blast shear* energy acting against the former two energies. When the capillary holding is weak for CWS containing large particles, or when the air blast energy is too strong to override the former two energies, coal particles easily separate from water and the resulting spray consists of nearly pure water droplets and CWS droplets containing a limited number of coal particles. As a result of this fine water spray, the overall mean drop diameter can significantly decrease with an increase in coal particle size.

Chapter 6 Suggestion for Future Research

Three suggestive ideas are listed for possible continuation of the present study in the future:

1. A systematic investigation can be made to study the effect of surfactant on the atomization performance of CWS sprays containing differently sized coal particles. This study will find out how largely the surfactant can contribute to enhance the CWS spray atomization in addition to the effect of coal particle sizes.
2. The use of size-classified glass beads or aluminum powder substituting coal particles is proposed to more rigorously study the effect of particle size on slurry atomization without incorporating hydraulic disintegration, dissolution, or surface adsorption.
3. An elaborate attempt can be made to atomize CWS mixtures containing higher weight fractions of classified coal particles. This will also require to examine the effect of the CWS viscosity on its atomization.

REFERENCES

1. G. D. Botsaris, and Y. M. Glazman, 1989, Interfacial Phenomena in Coal Technology, Marcel Dekker, New York, Chap. 3.
2. B. W. Brian, and J. C. Chen, 1987, "Surface Tension of Solid-Liquid Slurries," AICHE Journal, Vol. 33, No. 2, pp. 316-318.
3. K. D. Kihm, 1994, "Development and Use of an Apparatus to Measure the Dynamic Surface Properties of Coal-Water Slurry Fuels for Applications to Atomization Characteristics," DOE Report, Contract No. DE-FG-22-92PC92156.
4. R. Rosin and E. Rammler, 1933, "The Laws Governing the Fitness of Powdered Coal," Institute of Fuel, pp. 29-36.
5. R. C. Weast (ed.), 1988, CRC Handbook of Chemistry and Physics, CRC Press, Boca Raton, F-34.

LIST OF PUBLICATIONS UNDER THE DOE SUPPORT

1. K. D. Kihm, and P. Deignan, 1995, "Dynamic Surface Tension of Coal-Water Slurry Fuels," *Fuel*, Vol. 74, No. 2, pp. 295-300.
2. K. D. Kihm, G. M. Lyn, and S. Y. Son, 1995, "Atomization of Cross Injecting Sprays into Convective Air Stream," *Atomization and Sprays*, Vol. 5, Nos. 4&5, pp. 417-433.
3. K. D. Kihm, and P. Deignan, 1995, "Interfacial and Rheological Properties of Coal-Water Slurry (CWS) Fuels," *Proc. 20th International Technical Conference on Coal Utilization & Fuel Systems*, pp. 165-176, Clearwater, Florida.
3. K. D. Kihm, and P. Deignan, 1995, "Investigation of the Effect of the Coal Particle Sizes on the Interfacial and Rheological Properties of Coal-Water Slurry Fuels," *Proc 11th Annual Coal Preparation, Utilization, and Environmental Control Contractors Conference*, pp. 407-414, Pittsburgh, Pennsylvania.
4. K. D. Kihm, and G. M. Lyn, 1994 "Atomization of Cross Injecting Sprays into Convective Airstream," *Proc. Institute of Liquid Atomization and Spray System*, Bellevue, Washington, pp. 167-171.
5. K. D. Kihm, 1994, "Development and Use of an Apparatus to Measure the Dynamic Surface Properties of Coal-Water Slurry Fuels for Applications to Atomization Characteristics," DOE Report, Contract No. DE-FG-22-92PC92156.
6. K. D. Kihm, P. D. Deignan, and S. S. Kim, 1993, " Investigation of Dynamic Surface Tension of Coal Water Slurry (CWS) Fuels for Applications to Atomization Characteristics," *Proc. 18th Int. Tech. Conf. on Coal Utilization & Fuel Systems*, Clearwater, Florida, pp. 637-648.
7. K. D. Kihm, 1993, "Development and Use of an Apparatus to Measure the Dynamic Surface Properties of Coal Water Slurry Fuel," *Proc. 9th Annual Coal Preparation, Utilization, and Environmental Control Contractors Conference*, Pittsburgh, Pennsylvania, pp. 186-193.